END

DATE
FILMED

4-77

AFGL-TR-76-0294

(12)

THEORY OF ELECTRON EMISSION

EFFECTS IN SYMMETRIC PROBE

AND SPACECRAFT SHEATHS

Lee W. Parker

Lee W. Parker, Inc.
252 Lexington Road
Concord, Massachusetts 01742

D D C

MAR 31 1977

C

30 September 1976

Final Report for Period 1 November 75 - 30 June 76

REPORT DOCUMENTATION PAGE

READ INSTRUCTIONS
BEFORE COMPLETING FORM

1. REPORT NUMBER	2. GOVT ACCESSION NO.	3. RECIPIENT'S CATALOG NUMBER
AFGL-TR-76-0294		

4. TITLE (and Subtitle)	5. TYPE OF REPORT & PERIOD COVERED
THEORY OF ELECTRON EMISSION EFFECTS IN SYMMETRIC PROBE AND SPACECRAFT SHEATHS.	Final rept. 1 Nov 1975 through 30 Jun 76.
	6. PERFORMING ORG. REPORT NUMBER

7. AUTHOR(S)	8. CONTRACT OR GRANT NUMBER(S)
Lee W. Parker	F19628-76-C-0110 new

9. PERFORMING ORGANIZATION NAME AND ADDRESS	10. PROGRAM ELEMENT, PROJECT, TASK AREA & WORK UNIT NUMBERS
Lee W. Parker, Inc. 252 Lexington Road Concord, Massachusetts 01742	62101F 76610701

11. CONTROLLING OFFICE NAME AND ADDRESS	12. REPORT DATE
Air Force Geophysics Laboratory Hanscom AFB, Massachusetts 01731 Monitor/Paul L. Rothwell/PHE	30 September 1976
	13. NUMBER OF PAGES

14. MONITORING AGENCY NAME & ADDRESS(if different from Controlling Office)	15. SECURITY CLASS. (of this report)
	Unclassified
	15a. DECLASSIFICATION/DOWNGRADING SCHEDULE

16. DISTRIBUTION STATEMENT (of this Report)

Approved for public release; distribution unlimited.

17. DISTRIBUTION STATEMENT (of the abstract entered in Block 20, if different from Report)

D D C
MAR 31 1977

18. SUPPLEMENTARY NOTES

19. KEY WORDS (Continue on reverse side if necessary and identify by block number)

spacecraft
spacecraft potential
spacecraft plasma sheath
spacecraft photosheath

Langmuir probe
photoelectron emission
secondary-electron emission

computer plasma
plasma simulation
numerical analysis

20. ABSTRACT (Continue on reverse side if necessary and identify by block number)

A computer model developed earlier (Parker, 1975), for the rigorous theory of the steady-state sheath structure about and the particle fluxes to a conducting spherical body in a collisionless plasma, has been extended to include the contributions of emitted electrons in addition to those of the ambient plasma. The method is also extended to apply to long cylinders as well as to spheres. Potential barriers and general non-monotonic

DD FORM 1473 EDITION OF 1 NOV 65 IS OBSOLETE
1 JAN 73

391 800

potential distributions are taken into account. Solutions are possible
for wide ranges of the values of the relevant parameters, and are applic-
able to the sheaths and fluxes of emitting spacecraft, and to the current-
voltage characteristics of emitting Langmuir probes. The formulation for
the orbit analysis is based on the author's (1973, 1975) Turning-Point
function method, as opposed to the method of the Effective-Potential func-
tion exemplified by the work of Laframboise and Bernstein and Rabinowitz.
The two formulations have been shown by the author to be analytically
equivalent and to produce identical numerical results. However, in the
author's opinion the Turning-Point formulation is simpler and more effi-
cient than the Effective-Potential formulation.

Solutions are presented for a number of sample problems, using a code
PARKSS based on the analysis of this report. The discussion of these
solutions includes comparisons with previous theories and experimental
data. In these problems the effects are considered of variations of
(a) surface potential, (b) monoenergetic versus Maxwellian emission
velocity distributions, (c) emission flux relative to ambient fluxes
("weak" versus "strong" emission), and (d) emission temperature
relative to ambient temperatures ("cold" versus "warm" emission), on
potential barriers and net surface fluxes.

1. INTRODUCTION

This report is concerned with rigorous calculations of the structure of the charged-particle sheath about a symmetric body immersed in a plasma and emitting electrons from its surface. The body can be a space probe and the emission can consist of photoelectrons or secondary electrons. This becomes an important effect when the ambient plasma is hot and tenuous, say about a spacecraft outside the plasmasphere, and can influence electric field measurements (Grard et al, 1973) or low-energy particle experiments (Whipple and Parker, 1969). The model to be discussed is equally applicable to the problem of an electrostatic Langmuir probe in a laboratory plasma where the emitted electrons are thermionic or secondaries (Chang and Bienkowski, 1970).

Spherically-symmetric sheaths have been treated rigorously in the absence of emission by Laframboise (1966) and Parker (1975). The effects of emission on spherical bodies immersed in plasmas have been treated approximately by a number of workers (cf. Whipple, 1976 and references cited therein), but very little rigorous theoretical work has been reported. Schröder (1973) reports that he used the method of Laframboise (1966) to include photoelectrons, but gives no computational details. This is a significant omission because the Laframboise method is based on the assumption that the potential profile is monotonic whereas Schröder's results involve nonmonotonic potential profiles (potential minima), which would require a significant modification such as that of the present report.

There is ongoing work on dynamic time-simulation calculations for the spherical sheath problem (P. Rothwell, A. Wilson, private communications, 1976). These solutions have been found to agree (after the oscillations have become sufficiently small) with the author's static solutions (Parker, 1975 and this report) at sufficiently long times. However, certain difficulties are encountered with dynamic methods which are absent in static methods. For example, in seeking steady-state solutions one may find there are two or more different time-scales in the problem, which can make time-simulation relatively expensive. One may also inadvertently introduce

"numerical" collisions so that particles become inadvertently trapped, in a potential minimum for example. In addition, there may be excessive noise.

A rigorous spherically-symmetric model is needed, to provide relatively inexpensive but valuable guidance regarding the assessment of sheath structures in 3-dimensional problems. The present computer model, called PARKSS (Parker Spherical Sheath), has been developed with this aim. It is an extension of the author's previously developed computer model (Parker, 1975), but modified to take any nonmonotonic potential distribution into account. It should be mentioned that a time-simulation study by Soop (1972) for a conducting sphere illuminated on one side in a vacuum has shown that the asymmetry in the charge distribution is small. Hence, a spherically symmetric model should be a good approximation for the sheath around a spherical space probe. In addition, the problem of a long circular cylinder (which has clear implications for space, e.g., instrument booms, as well as laboratory applications) is so similar to that of a sphere that only slight modifications are required. Accordingly, the sphere and cylinder are treated on an equal basis in the analysis of this report.

In Section 2 the assumptions and basic foundations of the Vlasov problem are discussed. This refers to the evaluation of charged-particle densities and fluxes with arbitrary potential distributions. In Section 3, the solution of Poisson's equation, and the Poisson-Vlasov iteration procedure to obtain mutual consistency of the distributions of potential and charged-particle densities, are treated. The kinetic-theoretical problems of the evaluation of densities and fluxes are discussed in Sections 4 and 5, respectively. Here we consider Maxwellian and monoenergetic velocity distributions, for ambient and emitted particles, and for spheres and cylinders. The moment integrals are represented as integrals over energy and angular momentum. In Section 6 we consider the orbit analysis required to evaluate the angular momentum integrals. The formulation for this analysis is based on the Turning-Point function as opposed to the Effective Potential. The Turning-Point formulation is considered to be much simpler in practice and more efficient than the Effective-Potential formulation. The equivalence between the two formulations has been proved analytically and numerically (Parker, 1975), but is here demonstrated in one of several examples by

-2-

re-deriving on the basis of the Turning-Point formulation the formulas derived earlier by Bernstein and Rabinowitz (1959) who used the Effective Potential.

Section 7 and Appendix A are concerned with the energy-quadrature method wherein the moment integrals over energy are approximated by finite sums over monoenergetic factors. The method of Parker (1975) is here modified to deal with nonmonotonic potential distributions and arbitrary energy ranges which arise in the emission problem.

In Section 8, a number of sample spherical solutions obtained with the code PARKSS are discussed. The effects of (a) emitted electrons without the ambient plasma, (b) ambient plasma without emission, and (c) the combination of emitted electrons with the ambient plasma, are compared. When there is emission there is generally a negative potential minimum (or barrier) somewhere between the probe and infinity. Its qualitative behavior is as follows. For large positive surface potentials, the minimum has negligible depth and occurs at a large radius. As the surface potential is reduced, the minimum moves inward and becomes significantly deeper. At a negative value of surface potential, the minimum occurs at the surface, and at the surface the field is therefore zero. With more negative surface potentials the potential profile rises monotonically to zero. For positive surface potentials, the solutions are similar to those presented by Schröder (1973). However, there are some differences with Schröder's results. It is shown also that emission raises the equilibrium potential, as expected. The effects of strong versus weak emission (based on relative fluxes), and monoenergetic versus Maxwellian distributions of emission velocity, are compared. For weak and cold emission from a negative probe, the emitted electrons "run downhill," and their density falls rapidly and becomes asymptotically proportional to the inverse square of the radial distance. In a small-Debye-number probe problem, the point of quasineutrality, beyond which positive and negative charges balance to within a given small fraction, is unchanged by adding electron emission. Rigorous solutions are also obtained for a problem treated approximately by Whipple (1976) in attempting to interpret ATS-6 spacecraft data. The spherically-symmetric model was adopted to see whether potential barriers indicated by the data could be reproduced.

-3-

At various points throughout Section 8 equilibrium potentials are indicated. The limit of cold emission from a negative probe is derived in Appendix B.

The computer program PARKSS implementing the analysis of this report is presented in Appendix C.

2. FOUNDATIONS

The spacecraft is modelled by a conducting sphere or cylinder while the ambient plasma is isotropic, collisionless, and stationary with respect to the spacecraft. Photoelectrons and secondary electrons are assumed to be emitted isotropically from the spacecraft surface. In the case of a Langmuir probe the emission can consist of either thermionic electrons or secondaries due to bombardment. Magnetic field effects are neglected. Far from the probe or satellite, the distribution functions for electrons and ions in the ambient plasma are treated in the present report as either Maxwellians or monoenergetic. The same applies to the distribution function for emitted electrons at the surface. The problem is assumed to be independent of time. It is desired to calculate the spatial distributions of electric potential and of electron and ion densities, as well as the currents of ions and electrons exchanged between the probe and the environment. The basic problem assumes a fixed potential on the surface, but it is a natural extension to find the floating potential by solving a sequence of problems until current balance has been achieved.

In accord with the foregoing assumptions, a particle distribution function f (which is the density in phase space) satisfies the time-independent Vlasov equation,

$$\vec{V} \cdot \nabla f - \frac{q}{m} \nabla \phi \cdot \nabla_V f = 0 \tag{1}$$

This states that f, which is a function of the vector position $\vec{R}$ and of the vector velocity $\vec{V}$, is constant along an orbit in an electric field of potential $\phi(\vec{R})$, where q and m denote respectively the charge and mass of the particle. In Eq. (1), ∇ and ∇_V denote gradient operators with respect to position and velocity space, respectively.

Assuming one has solved Eq. (1) for f subject to the appropriate boundary conditions (the "Vlasov problem" - see Secs. 4-6), one may then obtain the particle density $N(\vec{R})$ at a point $\vec{R}$ by integrating f over velocity space:

$$N(\vec{R}) = \iiint f(\vec{R},\vec{V}) \, d^p\vec{V} \tag{2}$$

where $d^p\vec{V}$ represents a p-dimensional volume element of the velocity space. For the spherical problem p=3, while p=2 for the cylindrical problem. This integral represents the zero-th moment of the distribution. Similarly, one may obtain the flux or current density at a point $\vec{R}$ by defining V_n as the component of velocity of interest and integrating the product fV_n over velocity space (the first moment):

$$j(\vec{R}) = \iiint f(\vec{R},\vec{V}) \, V_n d^p\vec{V} \tag{3}$$

On a spherical or cylindrical surface, V_n becomes V_r, the radial component of velocity.

One may determine the local value of $f(\vec{R},\vec{V})$ at an arbitrary point $\vec{R}$, by considering the orbit of a particle arriving at $\vec{R}$ with the velocity $\vec{V}$. If the orbit is traced backwards and a point is eventually reached where f is known (namely, the "source" at the surface or at infinity), then the local value of f is identical to the known value at the source. If the orbit is found to be closed upon itself, its population can consist only of trapped particles which can have arrived there through a collisional mechanism. It is assumed here that the closed orbits if any are unpopulated (that is, f=0 for these). This assumption is usually made for tractability purposes, based on a plausibility argument (Laframboise, 1966; Whipple, 1976), but its ultimate justification is difficult and requires a quantitative collisional theory. Such a theory is available (Parker, 1973), but has not as yet been applied to the present sheath problem.

Since we have assumed isotropic sources at the surface and infinity, and since total energy is conserved along an orbit, the velocity distributions

can depend only on the particle energy at the source. Denoting by V_∞ the particle speed at infinity, and by V_S the particle speed at the surface, we may define distinct distribution functions for ambient and emitted particles, depending on the distributions at the respective sources:

$$f_i (\infty, \vec{V}_\infty) \equiv F_\infty (MV_\infty^2/2) \tag{4}$$

$$f_e (\infty, \vec{V}_\infty) \equiv F_\infty (mV_\infty^2/2) \tag{5}$$

$$f_s (\vec{R}_S, \vec{V}_S) \equiv F_S (mV_S^2/2) \tag{6}$$

Here the subscripts $\underline{i}$ and $\underline{e}$ refer to the ambient ions (of mass M) and electrons (of mass m), respectively, while subscript $\underline{s}$ refers to the surface-emitted electrons. The arguments of F_∞ and F_S are related to the total energy which is constant along orbits. Then the distribution function for the ions at any point $\vec{R}$ can be written:

$$f_i (\vec{R}, \vec{V}) = \delta_i (\vec{R}, \vec{V}) \, F_\infty (MV_\infty^2/2) \tag{7}$$

For the electrons, there are separate distribution functions, one describing the electrons from infinity (F_∞), and the other those from the surface (F_S):

$$f_e (\vec{R}, \vec{V}) = \delta_e (\vec{R}, \vec{V}) \, F_\infty (mV_\infty^2/2) \tag{8}$$

$$f_s (\vec{R}, \vec{V}) = \delta_s (\vec{R}, \vec{V}) \, F_S (mV_S^2/2) \tag{9}$$

with the subscripts e and s referring, respectively, to the electrons from infinity (ambient), and those from the surface. The "delta-factors" $\delta_{i,e,s}$ $(\vec{R}, \vec{V})$ contain the orbit information, that is, regarding whether the orbit connects with the appropriate source. Thus, $\delta_i = 1$ if the ion comes from infinity, while $\delta_i = 0$ if the ion comes from the probe surface. Similarly,

$\delta_e = 1$ and $\delta_s = 0$ if the electron comes from infinity, while $\delta_e = 0$ and $\delta_s = 1$ if the electron comes from the surface. That is, a non-zero value for δ signifies that the orbit is "occupied." Since the δ's are step-functions, and the F-functions are known (to be defined in Sec. 4), it is only necessary to locate the boundaries of the regions in velocity space associated with the two different types of particle sources. For the symmetric problems of interest (spheres and cylinders), the regions in velocity space will be found to be further subdivided according to types of orbits, such as those which contribute once due to a single pass through the radius of interest, and those which contribute twice because the particle reverses direction after passing the radius of interest, and then re-crosses the radius of interest. Thus, the δ-factors which do not vanish can take on the value 2 as well as unity, as will be shown in Sec. 6.

Finally, the relation between the local speed V and the speed at the source (V_∞ for ambient particles, and V_s for emitted particles) is given by the total-energy relations

Ambient Ions

$$\frac{MV^2}{2} + e\phi = \frac{MV_\infty^2}{2} + e\phi_\infty \tag{10}$$

Ambient Electrons

$$\frac{mV^2}{2} + e\phi = \frac{mV_\infty^2}{2} + e\phi_\infty \tag{11}$$

Emitted Electrons

$$\frac{mV^2}{2} + e\phi = \frac{mV_s^2}{2} + e\phi_s \tag{12}$$

where ϕ is the electric potential, ϕ_s is the electric potential at the surface, and ϕ_∞ is the potential at infinity assumed to be zero; Eq. (10) is written for singly-charged ions, and e is the signed electron charge.

-8-

3. POISSON'S EQUATION (CALCULATION OF POTENTIALS) AND ITERATION PROCEDURE FOR POISSON-VLASOV SOLUTION

The electric potential ϕ is obtained from the solution of Poisson's equation, which may be expressed in terms of the ambient-ion number density N_i, the ambient-electron number density N_e, and the surface-electron number density N_s:

$$\nabla^2 \phi = 4\pi e(N_s + N_e - N_i) \tag{13}$$

where e denotes the magnitude of the electron charge. It is convenient to write this equation in dimensionless form, and in terms of the radial coordinate appropriate to a sphere or cylinder, where the radius of the sphere or cylinder is denoted by r_0. In non-dimensionalizing, one may choose the ambient parameters N_0 and T_e as basic, where N_0 denotes the ambient-plasma number density and T_e denotes the ambient electron temperature. One also defines N_{so} as the surface-electron number density evaluated at the surface. Then for the <u>sphere</u> Poisson's equation may be expressed in terms of the following dimensionless variables:

r = radial coordinate divided by r_0

ϕ = electric potential divided by kT_e/e

n_i = ambient-ion density divided by N_0

n_e = ambient-electron density divided by N_0

n_s = surface-electron density divided by N_{so}

λ_D = ambient-electron Debye length $(kT_e/4\pi N_0 e^2)^{1/2}$ divided by r_0 (that is, the Debye number)

The resulting equation for the spherical problem may be written:

$$\frac{d^2(r\phi)}{dr^2} = \frac{r}{\lambda_D^2} \left[n_s \frac{N_{so}}{N_0} + n_e - n_i \right] \tag{14}$$

The form of the left-hand side implies that this equation is to be solved for $r\phi$, from which ϕ is obtained by division by r. Alternatively, one may non-dimensionalize by choosing as basic the emission parameters N_{so} and T_s, where T_s is the effective temperature of an emitted Maxwellian distribution. Then the equation may be expressed in terms of the same dimensionless variables except the following:

ϕ = electric potential divided by kT_s/e

λ_{DS} = surface-electron Debye length $(kT_s/4\pi N_{so}e^2)^{\frac{1}{2}}$
divided by r_o (that is, the Debye number
based on the surface emission)

Then the equation may be written:

$$\frac{d^2(r\phi)}{dr^2} = \frac{r}{\lambda_{DS}^2}\left[n_s + \frac{N_o}{N_{so}} n_e - \frac{N_o}{N_{so}} n_i \right] \tag{15}$$

Equations (14) and (15) refer to the spherical problem. For the corresponding cylindrical problem, one may write instead of Eq. (14):

$$\frac{d^2\phi}{du^2} = \frac{e^{2u}}{\lambda_D^2}\left[n_s \frac{N_{so}}{N_o} + n_e - n_o \right] \tag{16}$$

where the new variable u is defined by $u = \ln r$. Equation (15), based on the surface emission parameters, may be similarly replaced.

Equations (14)-(16) may be solved by differencing them on a set of grid points, in r for the sphere and in u for the cylinder, and solving the difference equations. The reason for choosing the forms of Eqs. (14)-(16) is that a simple second-difference operation may be employed, namely,

$$(r\phi)_{i-1} - 2(r\phi)_i + (r\phi)_{i+1} = (\Delta r)^2 (RHS)_i \tag{17}$$

centered at the i-th grid point r_i for the spherical problem, and

-10-

$$\phi_{j-1} - 2\phi_i + \phi_{j+1} = (\Delta u)^2 (RHS)_j \qquad (18)$$

centered at the j-th grid point u_j for the cylindrical problem. In Eqs. (17) and (18), the right-hand-side factors $(RHS)_i$ and $(RHS)_j$ denote, respectively, the values of the right-hand sides of Eq. (14) and Eq. (16), for example, evaluated at the center grid point; and Δr and Δu denote the interval of a uniform grid.

The "double-sweep" method of solution for such tri-diagonal systems of linear equations is well known (Varga, 1962, for example). Floating boundary conditions to represent the boundary condition at infinity, appropriate for electrostatic probe and satellite problems, and the solution for non-uniform grids, are treated in Parker (1975).

Given the method for evaluating the ion and electron densities (to be discussed in the next section), the numerical solution of the sheath problem requires that of two fundamental sub-problems, the "Poisson Problem" (this section) and the "Vlasov Problem" (next three sections). The Poisson Problem is solved to yield the potentials at the grid points when the charged-particle densities are given, and conversely, the Vlasov Problem is solved to give the charged-particle densities at the grid points when the potentials are given. For mutual consistency an iterative process is required.

A suitable procedure for the iteration is given by Parker and Sullivan (1974) and Parker (1975). In the procedure, one mixes successive iterates of the charge density (or alternatively the potential iterates). This means that one mixes a fraction (α) of the most recently computed charge-density distribution (RHS in Eqs. (17) and (18)) with the complementary fraction ($1-\alpha$) of the previously used charge-density distribution. For small Debye numbers, the fraction α must be small. There is an upper limit for α, and correspondingly a minimum number of iterations, such that convergence is assured. These depend on the type of boundary condition used to represent infinity, as well as on the number of Debye lengths between the surface and the outer grid boundary. It can be shown (a) that for small Debye numbers the number of iterations required is proportional to the square of the inverse Debye number, and (b) that no mixing is required for convergence if the boundary

of the grid is less than about π Debye lengths from the surface (Parker and Sullivan, 1974).

The boundary condition where the potential floats in accord with an assumed inverse-square-law behavior is physically appropriate (Laframboise, 1966) and is found to be computationally efficient for the purely-ambient-plasma problem (Parker and Sullivan, 1974). This condition is also being used provisionally in the present program.

4. THE VLASOV PROBLEM: CHARGED-PARTICLE DENSITIES

We first consider Maxwellian distributions, of emitted and ambient particles, for the spherical problem (subsections A1 and A2) and for the cylindrical problem (subsections B1 and B2). Then we consider corresponding monoenergetic distributions (subsections C and D). Ambient-particle examples have been previously derived by Laframboise (1966) and Parker (1973 and 1975).

A. MAXWELLIAN DISTRIBUTIONS-SPHERE

We will derive in detail the number-density integral in the spherical problem for emitted particles. The ambient-particle number density formula will be shown to follow easily from that of the emitted particles.

A1. Maxwellian Emitted Particles, Spherical Problem

The number-density integral for emitted particles at a radial position R in the spherical problem is conveniently written as a specialization of the velocity space in Eq. (2) with p=3 to spherical-polar velocity coordinates V, θ, and β, where V is the local speed, θ is the local polar angle with respect to the radial direction, and β is the local azimuthal angle. The velocity-space volume element is $d^3\vec{V} = V^2 dV\, d(\cos\theta) d\beta$, but because of the assumed isotropy the integration over β is trivial (yielding the factor 2π), and Eq. (2) in view of Eqs. (4) and (7) may be written:

$$N_s(R) = 2\pi \int_0^\infty F_s(mV_s^2/2)V^2 dV \int_{-1}^1 \delta \cdot d(\cos\theta) \qquad (19)$$
(sphere)

where δ denotes the "delta-factor" for the emitted particles ($=\delta_s$ in Sec. 2, but here the subscript is dropped), which depends on the nature of the orbits. There are in general three distinct ranges of integration. These are associated with three corresponding types of contributing orbits, "Type 1," "Type 2," and "Type 3" as are defined in Sec. 6. We defer further discussion of the orbits until Sec. 6.

For a Maxwellian distribution of emitted particles at the surface we have

$$F_s(mV_s^2/2) = (2)N_{so}\left(\frac{m}{2\pi kT_s}\right)^{3/2} \exp(-mV_s^2/2kT_s) \qquad (20)$$

where T_s is the Maxwellian emission temperature. The first factor of 2 in parentheses represents the doubling appropriate to a half-Maxwellian distribution at the surface. This is consistent with Chang and Bienkowski (1970) and Schröder (1973). At zero field, the angular integral in Eq. (19) has contributions from only a hemisphere of directions at the surface (involving outgoing particles only). This situation is in contrast with the ambient plasma in which there is a full Maxwellian at infinity (involving both outgoing and incoming particles, at zero field); in the ambient distribution corresponding to Eq. (20) the factor 2 is replaced by unity.

Alternatively, one might wish to consider the surface distribution to be a full Maxwellian, but in the absence of an infinite external potential barrier there would be an imbalance of outgoing and incoming particles just outside the surface, resulting in a discontinuous density function. This situation could probably be made consistent by applying suitable re-definitions, but such a procedure seems neither immediately obvious nor physically satisfying. In any case, the normalization chosen affects the relationship between the current and the density. The factor 2 in parentheses will be retained here for the emitted particles but will be deleted for the ambient particles.

With Eq. (20) for F_s, Eq. (19) becomes

$$N_s(R) = \frac{(2)2N_{so}}{\sqrt{\pi}} \left(\frac{m}{2kT_s}\right)^{3/2} \int_0^\infty \exp(-mV_s^2/2kT_s)V^2 dV \int_{-1}^1 \delta \cdot d(\cos\theta) \quad (21)$$

where V_s is connected to V by Eq. (12). It is desirable next to make use of the symmetry of the problem to convert the variables of integration V and θ to new variables, namely, total energy and angular momentum, both of which are conserved along the orbits. It is also desirable to nondimensionalize the variables. We write:

-14-

$$r = R/r_0, \qquad\qquad n_s = N_s/N_{so}$$

$$v^2 = mV^2/2kT_s, \qquad\qquad v_s^2 = mV_s^2/2kT_s \qquad\qquad (22)$$

$$\phi = e\Phi/kT_s, \qquad\qquad \phi_s = e\Phi_s/kT_s$$

and convert to dimensionless total energy, namely, Eq. (12) nondimensionalized through division by kT_s:

$$E = v^2 + \phi = v_s^2 + \phi_s \qquad\qquad (23)$$

and the square of the angular momentum, nondimensionalized through division by $2mr_0^2 kT_s$:

$$J^2 = \frac{R^2}{r_0^2} \frac{V^2}{(2kT_s/m)} \sin^2\theta = r^2 v^2 \sin^2\theta \qquad\qquad (24)$$

For the sphere the angular momentum is that about the center of the sphere, while for the cylinder (treated next) it is that about the axis. The advantage of converting to the new velocity-space variables (E, J^2) is that both are constants of the motion and completely characterize an orbit independent of the variation of r along that orbit. In an orthogonal r-E-J^2 space the orbits are thus straight lines parallel to the r-axis (Parker, 1975), and the orbit analysis is simplified.

Using Eqs. (23) and (24) to eliminate V and θ in favor of E and J^2, we obtain from Eq. (21):

$$n_s(r) = \frac{2}{\sqrt{\pi}} \exp(\phi_s) \int_0^\infty \exp(-E) dE \cdot M_{ns}(E) \qquad\qquad (25)$$
(sphere)

where $M_{ns}(E)$ is the spherical monoenergetic contribution to n due to energy E. This monoenergetic factor is given by

-15-

$$M_{ns}(E) = \frac{(2)}{2} \sqrt{E-\phi} \int_{-1}^{1} \delta \cdot (\cos\theta)$$
(sphere)

$$= \frac{(2)}{2} \int_{0}^{\sqrt{E-\phi}} \delta \cdot d[E-\phi-J^2/r^2]^{1/2} \tag{26}$$

(δ to be evaluated in Sec. 6)

which is comprised of the integral over J^2 with E fixed.

A2. Maxwellian Ambient Particles, Spherical Problem

The Maxwellian number-density integral for ambient particles at a dimensionless radial position r in the spherical problem is so similar to that of the emitted particles that the final expression can be obtained readily from Eqs. (25) and (26). Thus, we set ϕ_s=0 since it now represents the potential at infinity, delete the factor 2 in parentheses, and obtain, for either the ambient ions or the ambient electrons:

$$n_{amb}(r) = \frac{2}{\sqrt{\pi}} \int_{0}^{\infty} \exp(-E)dE \cdot M_{ns}(E) \tag{27}$$
(sphere)

where $M_{ns}(E)$ is the monoenergetic contribution of the energy E. This factor is

$$M_{ns}(E) = \frac{1}{2} \int_{0}^{\sqrt{E-\phi}} \delta \cdot d[E-\phi-J^2/r^2]^{1/2} \tag{28}$$
(sphere)

(δ to be evaluated in Sec. 6)

where we have defined:

$n_{amb} = N_{i,e}/N_0$ for ions, electrons

$\phi = e\phi/kT_{i,e}$ for ions, electrons

T_i, T_e = ambient-ion, ambient-electron, temperature

$E = (MV^2/2 + |e|\phi)/kT_i$ for ions

$E = (mV^2/2 - |e|\phi)/kT_e$ for electrons

$J^2 = (R^2/r_0^2)(MV^2 \sin^2\theta)/2kT_i$ for ions

$J^2 = (R^2/r_0^2)(mV^2 \sin^2\theta)/2kT_e$ for electrons

-16-

B.   MAXWELLIAN DISTRIBUTIONS-CYLINDER

We next consider Maxwellian distributions, of emitted and ambient particles, in the cylindrical problem.

B1.   Maxwellian Emitted Particles, Cylindrical Problem

The number-density integral for emitted particles at a radial position R in the cylindrical problem is obtained when one specializes the velocity space in Eq. (2) with p=2 to cylindrical velocity coordinates V and θ. Here V is the speed in the transverse plane perpendicular to the cylinder axis and θ is the (azimuthal) angle in the transverse plane, with respect to the radial direction. The velocity-space volume element is $d^2\vec{V}=VdVd\theta$, and Eq. (2) now becomes

$$N_s(R) = 2 \int_0^\infty F_s(mV_s^2/2kT_s)VdV \int_0^\pi \delta \cdot d\theta \qquad (30)$$
(cylinder)

where the "delta-factor" is identical to that of Eq. (19) for the sphere. For a Maxwellian distribution of emitted particles at the surface we have:

$$F_s(mV_s^2/2) = (2) N_{so}(\frac{m}{2\pi kT_s}) \exp(-mV_s^2/2kT_s) \qquad (31)$$

The considerations of a half Maxwellian versus a full Maxwellian discussed following Eq. (20) apply equally well here. The factor 2 in parentheses will be retained here for the emitted particles but will be deleted for the ambient particles. Equation (30), with Eq. (31), may be converted to $E-J^2$ space with variables nondimensionalized as in Eqs. (22)-(24), and we obtain

$$n_s(r) = \exp(\phi_s) \int_0^\infty \exp(-E)dE \cdot M_{nc}(E) \qquad (32)$$
(cylinder)

where $M_{nc}(E)$ is the cylindrical monoenergetic contribution to n due to energy E.

This factor is given by

-17-

$$M_{nc}(E) = \frac{(2)}{\pi} \int_0^\pi \delta \cdot d\theta$$
(cylinder)

$$= \frac{(2)}{\pi} \int_0^\pi \delta \cdot d \left\{ \sin^{-1}[J^2/r^2(E-\phi)]^{\frac{1}{2}} \right\} \tag{33}$$

(δ to be evaluated in Sec. 6)

which is comprised of the integral over J^2 with E fixed.

B2. Maxwellian Ambient Particles, Cylindrical Problem

The Maxwellian number-density integral for ambient particles at r in the cylindrical problem is obtained readily from Eqs. (32) and (33). Again, setting $\phi_s = 0$ and deleting the factor 2 in parentheses as in the spherical problem, we obtain, for either ambient ions or ambient electrons:

$$n_{amb}(r) = \int_0^\infty \exp(-E)dE \cdot M_{nc}(E) \tag{34}$$
(cylinder)

where $M_{nc}(E)$ is the monoenergetic contribution given by

$$M_{nc}(E) = \frac{1}{\pi} \int_0^\pi \delta \cdot d\{\sin^{-1}[J^2/r^2(E-\phi)]^{\frac{1}{2}}\} \tag{35}$$
(cylinder)

The dimensionless variables are defined by Eq. (29).

C. MONOENERGETIC DISTRIBUTIONS-SPHERE

It is sometimes convenient to approximate a Maxwellian distribution by an equivalent monoenergetic one (Laframboise, 1966) and for this reason the monoenergetic formulas are of interest.

C1. Monoenergetic Emitted Particles, Spherical Problem

For emitted particles in the spherical problem, it can be shown that the appropriate monoenergetic distribution is

$$F_s(mV_s^2/2) = \frac{(2)N_{so}}{2\pi} \left(\frac{m}{2K_o}\right)^{3/2} D(1-mV_s^2/2K_o) \tag{36}$$

where $D(x)$ is the Dirac delta-function, and K_o is the singular value of the kinetic energy at the source. Substituting Eq. (36), in place of the Maxwellian Eq. (20), into Eq. (19), and nondimensionalizing as in Subsection A1 (Eqs. (22)-(24)) but with the normalizing energy kT_s replaced by K_o, yields:

n_s (sphere, monoenergetic)

$$= \frac{(2)}{2} \int_0^{\sqrt{1+\phi_s-\phi}} \delta \cdot d[1+\phi_s-\phi-J^2/r^2]^{1/2} \tag{37}$$

This expression becomes identical to the monoenergetic factor Eq. (26) when E is replaced by $1+\phi_s$.

C2. Monoenergetic Ambient Particles, Spherical Problem

For **ambient** particles in the **spherical** problem, the monoenergetic number density is obtained readily from Eq. (37), by setting $\phi_s=0$ and deleting the factor 2 in parentheses. Thus:

n_{amb} (sphere, monoenergetic)

$$= \frac{1}{2} \int_0^{\sqrt{1-\phi}} \delta \cdot d[1-\phi-J^2/r^2]^{1/2} \tag{38}$$

where the dimensionless variables are defined by Eq. (29) but with kT_i or kT_e replaced by K_o.

D. MONOENERGETIC DISTRIBUTIONS-CYLINDER

In contrast to the spherical problem, it is doubtful if in the cylindrical problem it makes sense to approximate a Maxwellian distribution by an equivalent monoenergetic distribution confined to the transverse plane. However, the appropriate formulas are included here for completeness, without derivation.

n_s (cylinder, monoenergetic)

$$= \frac{(2)}{\pi} \int_0^\pi \delta \cdot d\{\sin^{-1}[J^2/r^2(1+\phi_s-\phi)]^{1/2}\} \tag{39}$$

n_{amb} (cylinder, monoenergetic)

$$= \frac{1}{\pi} \int_0^\pi \delta \cdot d\{\sin^{-1}[J^2/r^2(1-\phi)]^{1/2}\} \tag{40}$$

where all quantities have been previously defined.

5. THE VLASOV PROBLEM: CHARGED-PARTICLE CURRENTS (FLUXES)

The order in which the various types of currents (fluxes) are con-
sidered will follow that of the previous section on number densities.
Namely, we treat Maxwellian distributions of emitted and ambient par-
ticles for the spherical problem, and then the same for the cylindrical
problem. Following these, the corresponding monoenergetic distributions
will be considered.

A. MAXWELLIAN DISTRIBUTIONS-SPHERE

We derive here the flux of emitted particles in the spherical problem.
The ambient-particle flux will follow readily.

A1. Maxwellian Emitted Particles, Spherical Problem

The current or flux integral for emitted particles in the spherical
problem is given, in accord with Eq. (3) with p=3, by multiplying the inte-
grand of Eq. (19) by $V_r \equiv V\cos\theta$, the radial component of velocity. Thus,
the emitted flux may be written:

$$j_s(\text{sphere}) = \pi \int_0^\infty F_s(mV_s^2/2)V^3 dV \int_0^1 \delta \cdot d(\sin^2\theta) \qquad (41)$$

Here, the range of θ-integration is reduced by one-half, namely $(0,\pi/2)$,
since flux contributions occur only over a hemisphere of directions. With
F_s given by Eq. (20) for the Maxwellian, the analysis proceeds in a manner
similar to that for the density. The results are as follows:

$$j_s(\text{sphere, Maxwellian})$$

$$= (2)N_{so}\sqrt{\frac{kT_s}{2\pi m}} \exp(\phi_s) \int_0^\infty \exp(-E)dE \cdot M_{js}(E) \qquad (42)$$

where $M_{js}(E)$ is the monoenergetic contribution given by

$$M_{js}(E) = \int_0^{(E-\phi)} \delta \cdot d(J^2/r^2) \tag{43}$$

(where r~1 at the surface)

where all dimensionless quantities are defined in Sec. 4. The neutral flux (at zero field) is $(2)N_{so}\sqrt{kT_s/2\pi m}$.

A2. Maxwellian Ambient Particles, Spherical Problem

As in Sec. 4, we obtain the ambient-particle expression from the emitted-particle expression by (a) setting $\phi_s=0$, (b) deleting the factor 2 in parentheses, and (c) replacing the emission parameters by the corresponding ambient parameters. Thus we have

$$j_{amb}(\text{sphere, Maxwellian})$$

$$= N_0 \left\{ \begin{array}{c} \sqrt{kT_i/2\pi M} \\ \\ \sqrt{kT_e/2\pi m} \end{array} \right\} \cdot \int_0^\infty \exp(-E)dE \cdot M_{js}(E) \tag{44}$$

where the monoenergetic factor $M_{js}(E)$ is identical to that given by Eq. (43), and the upper and lower square-root factors belong, respectively, to the ambient ions and electrons. The neutral flux (at zero field) is $N_0\sqrt{kT/2\pi m}$.

B. MAXWELLIAN DISTRIBUTIONS-CYLINDER

B1. Maxwellian Emitted Particles, Cylindrical Problem

For the cylinder, we multiply the integrand of Eq. (30) by $V_r \equiv V\cos\theta$, the radial component of velocity. Then the cylinder emitted flux may be written:

$$j_s(\text{cylinder}) = 2 \int_0^\infty F_s(mV_s^2/2)V^2 dV \int_0^1 \delta \cdot d(\sin\theta) \tag{45}$$

where the range of θ-integration is again halved to reflect the restriction of directions to those contained in a hemicylinder. With F_s given by Eq. (31), we obtain:

-22-

j_S(cylinder, Maxwellian)

$$= (2)N_{so}\sqrt{\frac{2kT_S}{\pi^2 m}}\ exp(\phi_S)\ \int_0^\infty exp(-E)dE\cdot M_{jc}(E) \qquad (46)$$

where the monoenergetic contribution $M_{jc}(E)$ is given by

$$M_{jc}(E) = \int_0^{\sqrt{E-\phi}} s\cdot d(\sqrt{J^2/r^2}) \qquad (47)$$

(where r=1 at the surface)

The neutral flux (at zero field) is $(2)N_{so}\sqrt{kT_S/2\pi m}$.

B2. Maxwellian Ambient Particles, Cylindrical Problem

We obtain the ambient-particle expression from the emitted-particle expression as in Sec. A2 above. This yields:

j_{amb}(cylinder, Maxwellian)

$$= N_0 \left\{ \begin{array}{c} \sqrt{2kT_i/\pi^2 M} \\ \hline \\ \sqrt{2kT_e/\pi^2 m} \end{array} \right\} \cdot \int_0^\infty exp(-E)dE\cdot M_{jc}(E) \qquad (48)$$

where we take the upper square root for the ions and the lower for the electrons; $M_{jc}(E)$ is given by Eq. (47). The neutral flux (at zero field) is $N_0\sqrt{kT/2\pi m}$.

C. MONOENERGETIC DISTRIBUTIONS-SPHERE

Using the monoenergetic distribution Eq. (36) in Eq. (41) results in the following monoenergetic fluxes for the spherical problem:

j_s(sphere, monoenergetic)

$$= (2)N_{so}\sqrt{\frac{K_o}{8m}} \int_0^{(1+\phi_s-\phi)} \delta \cdot d(J^2/r^2) \tag{49}$$

(where r=1 at the surface)

for the emitted particles, and therefore

j_{amb}(sphere, monoenergetic)

$$= N_o \left\{ \begin{array}{c} \sqrt{K_o/8M} \\ \\ \sqrt{K_o/8m} \end{array} \right\} \cdot \int_0^{(1-\phi)} \delta \cdot d(J^2/r^2) \tag{50}$$

(where r=1 at the surface)

for the ambient ions and electrons, respectively. The neutral fluxes (at zero field) are $(2)N_{so}\sqrt{K_o/8m}$ and $N_o\sqrt{K_o/8m}$, respectively. Note that for the sphere the monoenergetic neutral flux is equal to the corresponding Maxwellian neutral flux if $K_o = 4kT/\pi$.

D.   MONOENERGETIC DISTRIBUTIONS-CYLINDER

We repeat here the statement of Sec. 4D that it seems to make no sense in the cylindrical problem to use a monoenergetic distribution in the transverse plane. However, the formulas are included for completeness.

j_s(cylinder, monoenergetic)

$$= (2)N_{so}\sqrt{\frac{2K_o}{\pi^2 m}} \int_0^{\sqrt{1+\phi_s-\phi}} \delta \cdot d(\sqrt{J^2/r^2}) \tag{51}$$

(where r=1 at the surface)

for the _emitted_ particles,

and

j_{amb}(cylinder, monoenergetic)

$$= N_0 \left\{ \begin{array}{c} \sqrt{2K_0/\pi^2 M} \\ \\ \sqrt{2K_0/\pi^2 m} \end{array} \right\} \cdot \int_0^{\sqrt{1-\phi}} \delta \cdot d(\sqrt{J^2/r^2}) \qquad (52)$$

(where r=1 at the surface)

for the <u>ambient</u> ions and electrons. For the cylinder, the monoenergetic
neutral flux becomes equal to the corresponding Maxwellian neutral flux if
$K_0 = \pi kT/4$.

6. THE VLASOV PROBLEM: ORBIT ANALYSIS

In Secs. 4 and 5 the monoenergetic contributions involved ranges of integration over angular momentum represented by "delta-factors" associated with these ranges. The delta-factors will be defined here in terms of the contributions of three types of orbits, namely, Types 1, 2, and 3 (Parker, 1973, 1975), as illustrated in Fig. 1.

Type 1

The Type-1 orbit passes from infinity to the sphere, one way, or from the sphere to infinity, one way, with no turning-point. The ingoing orbit is populated by a particle from the ambient plasma, while the outgoing orbit is populated by a particle emitted from the surface. For Type-1 orbits the delta-factor is unity.

Type 2

The Type-2 orbit starts at infinity and passes inward, to a minimum radius (radial turning-point) outside the sphere. It subsequently goes out again. These are two-way orbits, occupied by ambient particles going in either direction. For Type-2 orbits, the delta-factor is 2. (It is of course zero if the turning-point is outside the radius of interest.)

Type 3

The Type-3 orbit starts at the sphere surface and passes outward to a maximum radius (radial turning-point), subsequently returning to the sphere. These orbits, similar and inverse to the Type-2 orbits, are also two-way orbits; they are occupied by emitted particles going in either direction. For Type-3 orbits the delta-factor is 2. (It is of course zero if the turning-point is inside the radius of interest.)

Type 4

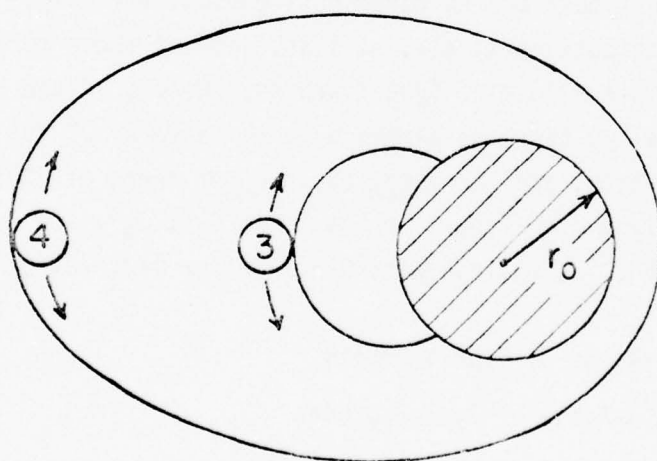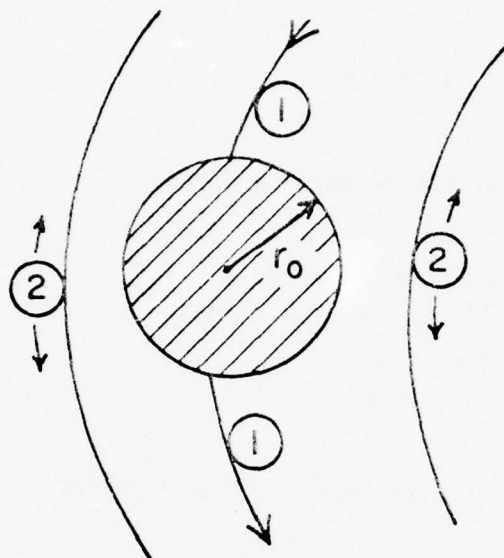This closed orbit is populatable by collisions. Examples are given by Parker (1973).

FIG. 1.   TYPES OF ORBITS

Consider a typical monoenergetic integral of Secs. 4 or 5. Denote its value by $M(E)$. Then it has the form:

$$M(E) = (const) \int \delta \cdot dG(J^2/r^2) \qquad (53)$$

where $G(X)$ is a function having various forms:

$G(X) = \sqrt{K-X}$ spherical density

$G(X) = \sin^{-1}\sqrt{X/K}$ cylindrical density

$G(X) = X$ spherical flux

$G(X) = \sqrt{X}$ cylindrical flux

where the total range of X is $(0,K)$. Here, X represents J^2/r^2 while K represents $E-\phi$.

The analysis of Parker (1973) shows that it is possible to have Type-1 and Type-2 orbits contributing simultaneously, or it is possible to have Type-1 and Type-3 orbits contributing simultaneously; but it is <u>not</u> possible to have Type-2 and Type-3 orbits contributing simultaneously. Moreover, if there are any contributions at all, at least some of these come from the vicinity of $J^2=0$ in the form of Type-1 orbits. Hence, if the point r can be reached energetically, there is <u>always</u> a <u>lower</u> range of J^2 for which there are only Type-1 orbits, and there <u>may</u> be an <u>upper</u> range of J^2 for which there are <u>either</u> Type-2 <u>or</u> Type-3 orbits. Let J_1^2, J_2^2, and J_3^2 denote critical values of J^2 as follows (with $0<J_1^2<J_2^2$ or $0<J_1^2<J_3^2$):

$(0,J_1^2)$=Range of Type-1 orbits

(J_1^2,J_2^2)=Range of Type-2 orbits $\qquad (54)$

(J_1^2,J_3^2)=Range of Type-3 orbits

At the surface, the flux and density can have contributions <u>only</u> from Type-1 orbits.

In terms of J_1^2, J_2^2, and J_3^2, the monoenergetic integral of Eq. (53) may now be written for <u>density</u>:

$$M(E) = (\text{const})|G(J_1{}^2/r^2)-G(0)+2G(J_m{}^2/r^2)-2G(J_1{}^2/r^2)|$$

$$= (\text{const})|-G(0)+2G(J_m{}^2/r^2)-G(J_1{}^2/r^2)|$$

(55)

where m=2 (Type-2 orbits) for ambient particles, and m=3 (Type-3 orbits) for emitted particles. The absolute-value signs take into account that G may be either an increasing or decreasing function. If there are only Type-1 orbits, then Eq. (55) is replaced by

$$M(E) = (\text{const})|G(J_1{}^2/r^2)-G(0)|$$

(56)

This equation always applies to _fluxes_. It may be obtained from Eq. (55) by setting $J_m{}^2 = J_1{}^2$.

Next, we consider how the critical values of J^2 are determined.

We write the equation for the conservation of energy in the dimensionless form

$$E = \phi + v_r{}^2 + J^2/r^2$$

(57)

where v_r denotes the radial component of velocity (in either the spherical or the cylindrical problem). Then along an orbit with fixed total energy E and fixed angular-momentum-squared $J,^2$ the radial velocity v_r will remain finite and will not vanish or change sign as long as the following inequality is satisfied:

$$E > \psi \equiv \phi + J^2/r^2$$

(58)

Alternatively, the inequality may be expressed by:

$$J^2 < g \equiv r^2(E-\phi)$$

(59)

Equation (58) may be analyzed to find the _maxima_ in the function ψ, which denotes the "effective potential." Alternatively, Eq. (59) may be analyzed to find the _minima_ in the function g, which denotes the "turning-point

function." The analyses of Eqs. (58) and (59) to classify the orbits represent, respectively, the methods of the Effective-Potential Formulation and the Turning-Point Formulation. The effective-potential approach is represented by the works of Bernstein and Rabinowitz (1959) and Laframboise (1966), while the turning-point approach is exemplified by the works of Bohm et al (1949), Allen et al (1957), Medicus (1961), and Parker (1973, 1975). The two approaches are of course equivalent (Parker, 1973, 1975). They involve different projections of the same 3-dimensional phase space of the variables r, E, and J^2. From the definition that v_r=o defines a turning-point, Eq. (57) with v_r=o defines a 3-dimensional surface representing the locus of turning-points. A <u>maximum of ψ</u> occurring in an r-E projection (at constant J^2) corresponds to a <u>minimum of g</u> occurring in an r-J^2 projection (at constant E) (Parker, 1975).

The Turning-Point Formulation is considered by the author to be much simpler in practice than the Effective-Potential Formulation, and has been shown to produce identical results (Parker, 1975). In using the Turning-Point Formulation to evaluate monoenergetic contributions (that is, contributions to the density or flux due to a given energy), one explores the g-function of Eq. (59) for least values (or minima) occurring in the radial range r=1 (the surface) to r=∞. For a fixed energy E there is only a single curve to analyze, such as that of each example in Fig. 2, which is an r-J^2 projection of the phase space.

Figure 2 shows 3 examples illustrating the use of the turning-point method, which depends on where and how least values ("negative bumps") occur in the g-function of Eq. (59). The least values may or may not be analytic minima. They correspond to "positive bumps" (representing centrifugal barriers) in the effective potential. In these examples E-φ is everywhere positive, but φ is otherwise arbitrary and in particular may be nonmonotonic. All physically possible orbits are horizontal lines constrained to remain below the function g=r^2(E-φ). Orbits terminating on the g-function have turning-points there.

We consider Case (A) in detail, and summarize all 3 cases in Table 1. There is one principal least value (minimum) in the g-function, at r=a, and no secondary least values. (This corresponds to an effective-potential

-30-
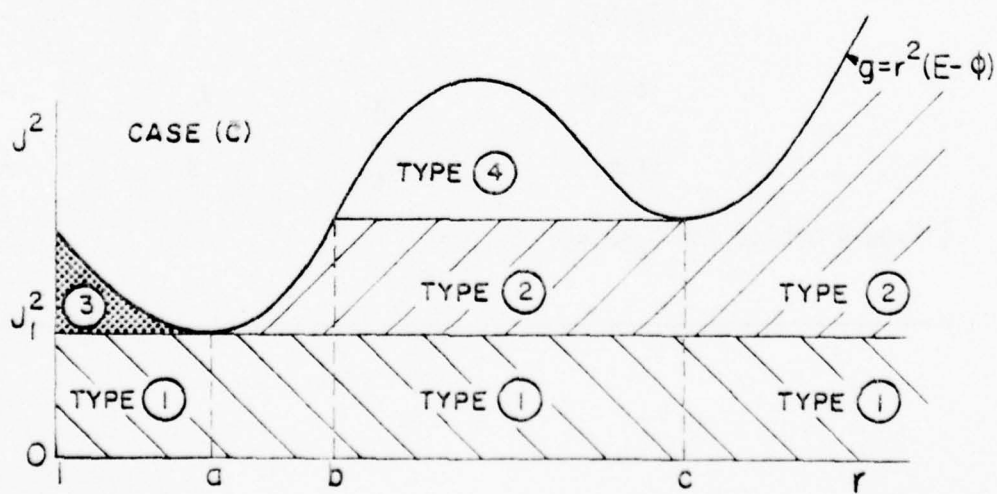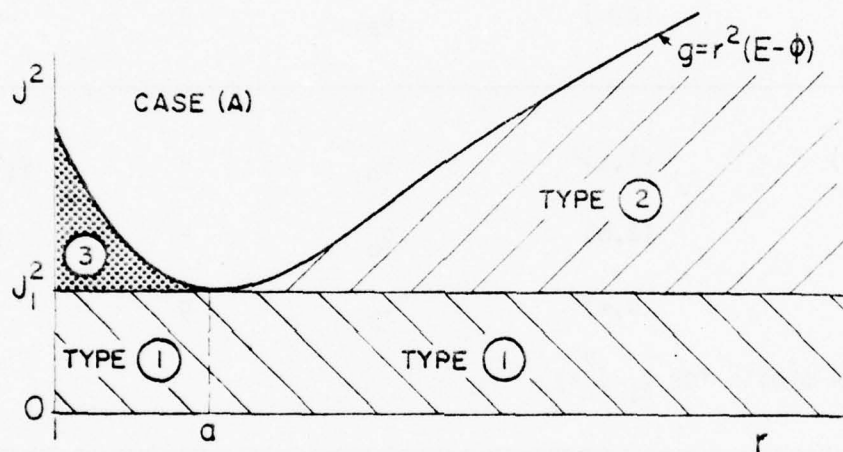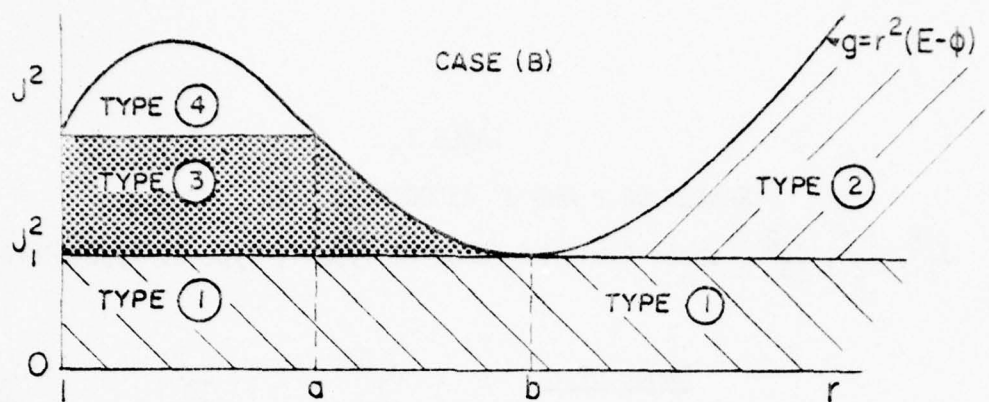
FIG. 2. TURNING-POINT METHOD, EXAMPLES

TABLE 1.

RANGES OF r AND J^2 ASSOCIATED WITH FIG. 2

J_1^2, J_2^2, J_3^2 = upper limit of range of Type-1, Type-2, Type-3 orbits

	Range of r	J_1^2	J_2^2	J_3^2
Case (A)	(1,a)	g_a	-	g
	(a,∞)	g_a	g	-
Case (B)	(1,a)*	g_b	-	$g_1 = g_a$
	(a,b)	g_b	-	g
	(b,∞)	g_b	g	-

(*Type-4 orbits for $g_1 < J^2 < g$)

Case (C)	(1,a)	g_a	-	g
	(a,b)	g_a	g	-
	(b,c)*	g_a	g_c	-
	(c,∞)	g_a	g	-

(*Type-4 orbits for $g_c < J^2 < g$)

function with a single maximum, at $r=a$.) At all positions r, the range of Type-1 orbits is (o, g_a), where $g_a \equiv g(r_a) \equiv J_1^2$, and J_1^2 is the upper limit of J^2 for Type-1 orbits in accord with Eq. (54). For r between $r=1$ and $r=a$, Type-3 orbits occur for J^2 in the range $J_1^2 < J^2 < g$, so that $J_3^2 = g$; there are no Type-2 orbits. For $r > a$, Type-2 orbits occur for J^2 in the range $J_1^2 < J^2 < g$, so that $J_2^2 = g$; there are no Type-3 orbits. The foregoing may be summarized as in Table 1.

Cases (B) and (C) have secondary minima (that of Case (B) is a least value occurring at $r=1$), in addition to the principal minimum. In all cases, Type-3 orbits can occur only to the left, and Type-2 only to the right, of the principal minimum. In Case (B), for r between 1 and a, the upper limit for Type-3 orbits is determined by the secondary minimum g_1 at $r=1$ rather than by the local value of g; in this range of r, values of J^2 above g_1 but less than g are associated with closed orbits (Type-4), as noted by the asterisked note in the table. Similarly, in Case (C), for r between b and c, the upper limit for Type-2 orbits is determined by the secondary minimum g_c at $r=c$ rather than by the local value of g; in this range of r, values of J^2 above g_c but less than g are associated with closed orbits (Type-4), noted in Table 1. A blank entry in the J_2^2-column of Table 1 means that there are only Type-1 orbits for the ambient particles, while a blank entry in the J_3^2-column means that there are only Type-1 orbits for the emitted particles. In either of these cases, Eq. (56) applies rather than Eq. (55).

It is evident from Fig. 2 that the existence of closed orbits is associated with the existence of secondary minima in the turning-point function (g).

The cases where g becomes negative in one or more ranges of r will be treated later.

Having determined J_1^2, J_2^2 (Type-2 orbits), and J_3^2 (Type-3 orbits) in Table 1 for the example cases of Fig. 2, we next show how they are used in the monoenergetic density and flux factors of Secs. 4 and 5.

Thus, we may now write down the monoenergetic formulas for density and flux, for ambient and emitted particles, for the sphere and cylinder. These

-33-

formulas are given by Eqs. (28), (43), (35), and (47), for the spherical density, spherical flux, cylindrical density, and cylindrical flux, respectively. In the following equations, we set m=1 if there are only Type-1 orbits. Otherwise, we set m=2 if the particles are ambient and there are Type-2 orbits, and we set m=3 if the particles are emitted and there are Type-3 orbits. Moreover, the factor C is unity for ambient particles and 2 for emitted particles.

Density, Sphere

$$M_{ns}(E) = \frac{C}{2} \int \delta \cdot d[E-\phi-J^2/r^2]^{\frac{1}{2}}$$

$$= \frac{C}{2} \left| \sqrt{E-\phi} - 2\sqrt{E-\phi-J_m^2/r^2} + \sqrt{E-\phi-J_1^2/r^2} \right| \tag{60}$$

Flux, Sphere

$$M_{js}(E) = \int_0^{E-\phi} \delta \cdot d(J^2/r^2) = J_1^2/r^2 = J_1^2 \tag{61}$$

since the flux of interest is at r=1.

Density, Cylinder

$$M_{nc}(E) = \frac{C}{\pi} \int_0^\pi \delta \cdot d\{\sin^{-1}[J^2/r^2(E-\phi)]^{\frac{1}{2}}\}$$

$$= \frac{C}{\pi} \left| 2\sin^{-1}\sqrt{J_m^2/r^2(E-\phi)} - \sin^{-1}\sqrt{J_1^2/r^2(E-\phi)} \right| \tag{62}$$

Flux, Cylinder

$$M_{jc}(E) = \int_0^{\sqrt{E-\phi}} \delta \cdot d(\sqrt{J^2/r^2}) = \sqrt{J_1^2/r^2} = \sqrt{J_1^2} \tag{63}$$

Note that the flux formulas are the same for emitted and ambient particles.

-34-

As a well-known example of the use of the foregoing formulas, we apply them to the problem considered by Bernstein and Rabinowitz (1959), namely, a spherical probe with monoenergetic ambient attracted particles. The potential falls off rapidly and monotonically, and the turning-point function has a form similar to that of Case (A) in Fig. 2, namely, a simple minimum. (This corresponds to a simple maximum in the effective-potential function studied by Bernstein and Rabinowitz.) Using Table 1 and Eqs. (60)-(63), we obtain the following results.

Density, Sphere $M_{ns}(E)$=:

$$\frac{1}{2}\left[\sqrt{E-\phi} - \sqrt{E-\phi-g_a/r^2}\right] \quad \text{for } r \text{ in } (1,a)$$

$$\frac{1}{2}\left[\sqrt{E-\phi} + \sqrt{E-\phi-g_a/r^2}\right] \quad \text{for } r \text{ in } (a,\infty)$$

(64)

Flux, Sphere

$$M_{js}(E)=g_a \tag{65}$$

Density, Cylinder $M_{nc}(E)$=:

$$\frac{1}{\pi}\sin^{-1}\sqrt{g_a/r^2(E-\phi)} \quad \text{for } r \text{ in } (1,a)$$

$$1 - \frac{1}{\pi}\sin^{-1}\sqrt{g_a/r^2(E-\phi)} \quad \text{for } r \text{ in } (a,\infty)$$

(66)

Flux, Cylinder

$$M_{js}(E)=\sqrt{g_a} \tag{67}$$

The foregoing equations for density and flux, Eqs. (64)-(67), are seen to be identical except for notation to those derived by Bernstein and Rabinowitz on the basis of the effective-potential formulation. The minimum of g occurs at r=a, which is the so-called "absorption radius," within which only Type-1 (one-way) orbits contribute to the density (and flux).

-35-

Another example which is even simpler is the ideal Langmuir limit ("orbit-limited"), in which the potential falls off less rapidly than the inverse-radius-squared. In this case, the g-function for an attractive potential rises monotonically from its value $E-\phi_0$ at the surface (not shown in Fig. 2). Then $J_1^2 = E-\phi_0$ and $J_2^2 = g$ for ambient particles. The spherical and cylindrical fluxes are $E-\phi_0$ and $\sqrt{E-\phi_0}$, respectively; here we have used Eqs. (65) and (67), respectively, with g_a replaced by $E-\phi_0$. This value of g_a can be used in the second member of Eq. (64) or Eq. (66) to yield the orbit-limited spherical and cylindrical density, respectively. For zero potential, we have $g_a = E$ and $\phi = 0$, so that we obtain the familiar forms $\sqrt{E}(1 + \sqrt{1-1/r^2})/2$ and $1-\pi^{-1} \sin^{-1}(1/r)$ for the spherical and cylindrical neutral density, respectively. (For the purely monoenergetic case E is replaced by unity; otherwise, with the factor $\sqrt{E}$ the integral over E gives unity.)

Finally, a numerical algorithm suitable for the computer to evaluate J_1^2, J_2^2, and J_3^2 is the following. We define g_i at a set of discrete grid points at radii r_i, where the potentials are ϕ_i, by $g_i = r_i^2(E-\phi_i)$. Here, i=1 denotes the surface radius. Then the computer is asked to find three types of least values of the g_i-array, namely:

$$J_1^2 \equiv \text{least } \{g_i\}, \text{ all } i$$

$$J_2^2 \equiv \text{least } \{g_j\}, \text{ all } j \geq i \tag{68}$$

$$J_3^2 \equiv \text{least } \{g_j\}, \text{ all } j \leq i$$

The case where g is negative over any range of r, as would occur at low values of E with a repulsive potential, is treated by setting $J_1^2 \equiv 0$. In addition, for ambient particles we set $M_n(E)=0$ at r if g vanishes anywhere between r and infinity; while for emitted particles we set $M_n(E)=0$ at r if g vanishes anywhere between r and the surface.

Whereas the program of Laframboise (1966) handles no more than two bumps in the effective potential, the present program (PARKSS - See Appendix C) can treat any number of bumps in the turning-point function. Thus, the method of this report is completely general, and applies not only to

-36-

nonmonotonic as well as monotonic potential distributions, but to completely general distributions.

7. ENERGY QUADRATURES

In order to evaluate numerically the integrals over energy in Secs. 4 and 5, one may employ quadrature formulas in the form:

$$\int_{E_{min}}^{\infty} \exp(-E)dE \cdot M(E) = \sum_{k=1}^{K} C_k \cdot M(E_k) \tag{69}$$

where $M(E)$ denotes the monoenergetic factor dependent upon energy E, and the lower limit E_{min} may be negative. In the sum there are K coefficients C_k and abscissas (energies) E_k, with k=1,2,...,K. The coefficients and abscissas depend on the order K and nature of the quadrature scheme chosen; those used in the present work are derived in Appendix A.

This section completes the analytical basis for a computer program. Numerical results are presented next.

8. SAMPLE RESULTS AND DISCUSSION

A computer program named PARKSS (for Parker Spherical Sheath) has been developed to implement the analysis of this report pertaining to the spherical problem. This section presents the results of a number of solutions. The numerical parameters (FORTRAN input in PARKSS code) include (a) RB ($=r_B$) = outer grid radius divided by the probe radius, (b) NMP = the number of grid points including the first and last in the interval $(1, r_B)$, and (c) ME = one-half the number of energies in the semi-infinite range. (There are also 2 (NMP-1) additional values of energy in the finite range - see Appendix A.) The 3 parameters RB, NMP, and ME must be large enough to ensure that the solution becomes insensitive to their values. One also needs to assign the value of ALPHA, the iteration parameter controlling the mixing of successive iterates.

For almost all of the runs, RB was set equal to 2, NMP was 21, ME was 5 (resulting in 50 energy-values), and ALPHA was 0.1. Except for emission-alone cases (for which the Dirichlet condition $\phi=0$ was used), the inverse-square-law floating boundary condition was employed at the outermost grid point in all cases. The results will be discussed with reference to specific figures and tables.

A. Figure 3 and Tables 2-4

Figure 3 shows three sets of dimensionless potential (ϕ) profiles: ambient plasma alone with no emission (curves labelled "A" on left side of Fig. 3), emitted electrons alone with no ambient plasma (curves labelled "E" on left side of Fig. 3); and both ambient and emitted (unlabelled curves on right side of Fig. 3). The profiles in Fig. 3 are associated with five values of the surface potential (ϕ_0), namely, 0.8, 0.4, 0., -0.4, and -0.8, corresponding to different vertical positions in the figure as indicated by the encircled numbers. Both the ambient and emitted thermal fluxes (Maxwellian) are assumed equal, corresponding to equal ambient and photoelectron fluxes, a condition which can occur in the plasmasphere (Grard et al, 1973). In particular, the temperatures of the plasma ions and electrons (T_i, T_e), of the emitted electrons (T_s), are assumed to be all equal

to one electron-volt; and the density of plasma ions and electrons (N_0) is equal to the emission density of photoelectrons (N_{so}), and both are taken equal to 400/cm³. Thus, the ambient and emitted thermal currents are both about 2×10^{-9} amp/cm², this being approximately the photoemission current. Thus, for a sphere radius of 100cm, the Debye number is 0.37.

Referring to the pure-ambient profiles (A in Fig. 3), we see that ϕ is always monotone and the profile for surface potential ϕ_0 is the negative of the profile for $-\phi_0$. Adding emission pushes the ϕ-profiles downward toward negative values, and the profiles are then possibly nonmonotonic. For ϕ_0 large and positive, ϕ falls off more rapidly while for ϕ_0 large and negative, ϕ falls off more slowly, than in the corresponding pure-ambient case.

The pure-emission profiles (E in Fig. 3) are similar to the combined-case profiles (ambient plus emitted), and both have the following features:

For ϕ_0 large and positive, ϕ is monotone downward, essentially out to infinity. However, there is always a negative minimum (potential "barrier"), which moves inward from infinity and becomes deeper as ϕ_0 becomes less positive. Numerically, it is difficult to "see" this barrier until ϕ_0 drops below about unity.

For $\phi_0 = 0$, we have a "pure" barrier, of height (or depth) about 3 units for emission only and under 2 units for the combined case.

There is a critical negative value of ϕ_0 such that the field vanishes at the surface. This is associated with the barrier having arrived at the surface. The critical value is about -0.8 for emission only and about -0.4 for the combined case. For ϕ_0 above the critical value, the surface electrons are pushed inward. Whereas for ϕ_0 below the critical value, the surface electrons are pushed outward; in this case, the potential is monotone upward and electrons emitted from the surface "roll downhill." In a sense, one may think of the barrier as a virtual one which has moved to within the surface.

Comparing the ambient-alone (A) and emitted-alone (E) profiles with the combined-case profiles, the latter appears roughly to be approximable by simply averaging the A and E profiles.

Table 2 presents dimensionless fluxes of plasma ions (j_i' and j_i), and plasma electrons (j_e) as functions of the surface potential (ϕ_0), in the Maxwellian ambient-only case. Here:

j_i' = ion flux normalized to ambient-ion thermal flux

j_i = ion flux normalized to ambient-electron thermal flux, assuming hydrogen ions and mass ratio M/m=1836

j_e = electron flux normalized to ambient-electron thermal flux

Note that j_i' (ϕ_0) = j_e ($-\phi_0$), and that equilibrium ($j_i=j_e$) occurs for ϕ_0 less than -2.

Table 3 presents dimensionless escaping-electron flux (j_s) as a function of the surface potential (ϕ_0), in the Maxwellian emission-only case. j_s is normalized by the emitted flux. As ϕ_0 decreases from +2, j_s increases until it becomes unity (all electrons escaping) when ϕ_0 passes the critical (zero-surface-field) value, which is at about -0.8. Also shown is ϕ_{min}, which denotes the (barrier) potential minimum, while r_m denotes the position of the minimum in sphere radii. One can see that the minimum moves inward and becomes deeper as ϕ_0 decreases from positive toward negative values. At $\phi_0=0$, the minimum is -0.28. There is no equilibrium surface potential for Maxwellian emission-only, as there would be for the monoenergetic emission-only case.

Table 4 presents dimensionless fluxes, of plasma ions (j_i' and j_i), of plasma electrons (j_e), and of escaping photoelectron flux (j_s), as functions of the surface potential (ϕ_0), in the combined case. Here, j_i, j_e, and j_s are all normalized by the emitted flux (which in this case is the same as the ambient-electron thermal flux). j_i' has the same definition as in Table 2. Table 4 is qualitatively similar to Table 3. j_s increases as ϕ_0 decreases until ϕ_0 passes the critical value, which is at about -0.2, as compared with -0.8 in the emission-only case. At $\phi_0=0$, the minimum is -0.12, as compared with -0.28 in the emission-only case. However, the radial position of the minimum is unchanged, at 1.35. The equilibrium surface potential is at ϕ_0 slightly above zero, compared with less than -2 in the ambient-only case.

The numbers of iterations required to achieve convergence of the potential-iterates to one part in 10^5 was 50-60 for the ambient-alone, 70-100 for the emitted-alone, and 40-100 for the combined cases.

B. Figures 4 and 5, and Table 5

Figures 4 and 5 are for a combined problem with both ambient plasma and emitted electrons, but where the emission is monoenergetic instead of Maxwellian. The plasma temperatures are $T_i=T_e=5eV$, while the emission temperature is $T_s=1eV$; the plasma and emission densities are $N_0=1/cm^3$ and $N_{so}=211/cm^3$, respectively. The plasma conditions are typical of those in the solar wind (Grard et al, 1973), while the emitted current corresponds to photoemission, about 10^{-9} amp/cm^2. This is a case of "strong emission," defined by $N_{so}\sqrt{T_s}$ $>>N_0\sqrt{T_e}$, that is, the emission flux (j_{so}) is much larger than the ambient-electron thermal flux (j_{eo}). For $r_0=100cm$, the emission Debye number is $\lambda_{DS}=0.51$, while the ambient-electron Debye number is $\lambda_{Do}=16.6$.

In Table 5, ϕ_0 is the dimensionless surface potential based on T_s, whereas the dimensionless fluxes of ions (j_i), of plasma electrons (j_e), and of escaping photoelectrons (j_s), are normalized with respect to the emission flux. Qualitatively, this table is roughly similar to Table 4, but there are some striking differences. The equilibrium ϕ_0 is very slightly below unity. For this case of strong monoenergetic emission it turns out to be very difficult to obtain numerical solutions very close to $\phi_0=1$, namely, in the range between the entries $\phi_0=0.99$ and $\phi_0=1.075$ of the table.

For ϕ_0 above unity:

(a) All emitted electrons return to the surface, and are contained within a radius $r(n_s=0)$.

(b) There is no minimum; the potential is strictly monotone.

(c) The position beyond which there are no emitted electrons, denoted by $r(n_s=0)$, within which all emitted electrons are contained, moves inward toward the surface with increasing ϕ_0 above unity.

As ϕ_0 drops below unity, there is a minimum which moves inward from infinity and becomes deeper. The minimum attains a depth of -.40 at ϕ_0=0, and the condition of zero field occurs at ϕ_0 between ϕ_0=-.5 and ϕ_0=-1.

Figure 4, where ϕ_0=0.99 (close to the equilibrium value), shows the potential profile (dashed curve labelled "ϕ") and the profiles for dimensionless plasma-ion density (n_i), plasma-electron density (n_e), and emitted-electron density (n_s). The density profiles are the solid curves. The emitted-electron density is 1.99 at the surface, since almost all emitted electrons return. The plasma-ion and plasma-electron densities remain close to one another, cross over, and essentially approximate to the neutral density (density at zero potential), shown as the dotted curve labelled "NEUTRAL". Hence, the ambient plasma seems to contribute little to the space charge.

The potential profile in Fig. 4 actually has a minimum of -0.0072 at r=1.95 (Table 5), but this is negligible in the scale of the figure.

Figure 5 shows the same profiles as Fig. 4, but for the larger positive surface potential ϕ_0=+2.0. This is in the regime where all emitted electrons return (n_s=2.0 at the surface) and are contained within the radius r=1.42. This datum is indicated in the second row of entries in Table 5. The interesting feature is that $n_s(r)$ approaches zero with infinite slope, at the position where ϕ=1.0 (where the electron speed vanishes). In this case, n_i and n_e are somewhat more separated than in the ϕ_0=.99 case. This case was used to make comparisons with a time-simulation calculation in which ϕ_0=+2 was found to occur during a very slow transient following a rapid one (P. Rothwell, private communication, 1976).

Runs were also made (not shown) in which the emission was Maxwellian instead of monoenergetic, with qualitatively similar results. One of the changes which occur, however, is that finite but negligible potential minima occur at large distances for large positive ϕ_0.

This problem is related to that of Schröder (1973) in being appropriate to a spherically-symmetric photoemissive space probe in the solar wind. Schröder computed a number of potential and density distributions, corresponding to different surface potentials and different plasma densities, for

a positively-charged probe. The computational method used is claimed to follow that of Laframboise (1966) but no details are given. (The Laframboise method is designed for monotonic potentials only.) Schröder's results show the features indicated in Tables 4 and 5, and Fig. 3, in that the potential minimum moves inward and becomes deeper as the positive surface potential decreases. However, whereas Schröder's curves for electron density move monotonically downward with increasing ϕ_0, it is found in present calculations that the density at a given r rises to a maximum and then falls off. Schröder also implies that the electron density falls off with the inverse-square of the radius at large radii. This is not found to be valid here for positive surface potentials, but it is valid for negative potentials and cold emission, as in the next problem.

The numbers of iterations required for individual solutions of this problem were in the range 50-100.

C. Figure 6

The problem of Fig. 6 again a combined ambient-emitted one, but is complementary to the previous problem in that the emission here is "weak" rather than strong. That is, the emission flux (j_{so}) is much smaller than the ambient-electron thermal flux (j_{eo}). Moreover, the ambient-electron temperature and density are T_e=1eV and N_0=100/cm^3, while the emitted-electron temperature T_s is vanishingly small in the sense that T_s/T_e is infinitesimal. Thus, the emission is "cold" as well as weak. The ambient-electron Debye number is 0.743 for a sphere radius of 100 cm. It is assumed for the purposes of Fig. 6 that the emission flux is one-tenth of the ambient-electron thermal flux (j_{so}/j_{eo}=0.1), and that the ions are unperturbed. Thus, the equilibrium potential for this problem is ϕ_0=-2.3. (The ion motions were included in similar problems not shown here, but were excluded for this problem to allow a comparison with an independent time-simulation calculation (A. Wilson, private communication, 1976). Including the ion motions moves the equilibrium potential up to about -1.8, but the qualitative behavior of the curves is the same.) The assumed values of the parameters can occur in the solar wind, but with reduced solar illumination, say at dawn or dusk.

-44-

In Fig. 6 the ϕ-distribution at the equilibrium potential is shown as a dashed curve (ϕ is the potential normalized by kT_e/e). The solid curves are for both types of electron density, with N_e/N_0 denoting the dimensionless plasma-electron density, and N_s/N_0 denoting the emitted-electron density normalized by N_0. The emitted-electron density due to cold emission may be shown (Appendix B) to be given by the formula

$$\frac{N_s(r)}{N_0} = \frac{1}{2\sqrt{\pi}\ r^2}\ \frac{j_{so}}{j_{eo}}\ \frac{1}{\sqrt{\phi(r)-\phi_0}} \tag{70}$$

which corresponds to electrons rolling downhill. The numerical factor becomes $1/20\sqrt{\pi}$ for $j_{so}/j_{eo}=0.1$. This formula also indicates that N_s/N_0 becomes infinite at the surface, which is consistent with the assumption of cold emission. Asymptotically, the density drops as r^{-2}.

About 70 iterations were required for this problem.

D.   Figure 7

Figure 7 shows the effects of adding surface emission to a probe problem treated earlier by the author (Parker, 1975) which involved only the ambient plasma. In the earlier problem, the dimensionless potential and Debye number were $\phi_0 = -10$ and $\lambda_D = 0.1$, respectively. In Fig. 7 the ambient-only curves of potential (ϕ) and density (n_i, n_e) are labelled "A", to be compared with the unlabelled corresponding curves including emission (n_s). The emission density and temperature are assumed to be the same as the ambient values (equal emission and ambient fluxes), and all 3 distributions are Maxwellian. This situation can occur in the plasmasphere if the spacecraft is several meters in radius. (To bring the equilibrium potential down to -10 would probably also require the use of an on-board electron gun.) The same situation can also occur in the laboratory with a small Langmuir probe emitting thermal or secondary electrons. The curves labelled "A" have been presented in an earlier report (Parker, 1975). The changes due to emission are characterized by the unlabelled curves, as follows:

-45-

(1) The ϕ-distribution is shifted upward slightly (in the negative direction).

(2) The ion density is raised about 10 percent near the surface, but the effect on the ions is insignificant beyond about 1.4 sphere radii.

(3) The plasma-electron density is reduced at all radii.

(4) However, the quasineutrality point beyond which the positive and negative charges balance ($n_i = n_e + n_s$) to within one percent is still at about the same radius (about 2 radii) as in the ambient-alone case.

(5) The emitted-electron density (n_s) drops off very rapidly at first, and asymptotically with the inverse square of the radius. This behavior is associated with electrons rolling downhill, and is characteristic of the "cold emission" treated in the previous problem, where $|e\phi_o| >> kT_s$.

With RB=3, NMP=41, and ALPHA=0.01, about 500 iterations were required. (By comparison, about 300 iterations were required when RB, NMP, and ALPHA were 2, 21, and 0.02, respectively.)

E. Table 6

In an attempt to interpret data obtained by instrumentation on the ATS-6 spacecraft, Whipple (1976) hypothesized the existence of a potential barrier due to secondary electrons or photoelectrons. In order to study this effect, Whipple assumed a spherically-symmetric model for the sheath as in the present report. However, his method was approximate in that (a) simplifications were assumed for the shapes of the boundaries in velocity space, i.e., the critical values of angular momentum (see Table 1), and (b) the method searched only for the most negative values of ϕ such that simultaneously $d\phi/dr=0$. The latter procedure is not likely to yield physically valid solutions since the boundary condition at infinity is ignored; however, it may be expected to provide an upper bound for the depth of the barrier potential. The former procedure (simplifications in velocity space) should be justified by exact theory such as the present one.

-46-

Table 6 is concerned with the 4 days (Days 198, 199, 204, and 273) defined in Whipple's paper. The ambient and emission data for the 4 days are given by the dimensional quantities (N_o, N_{so}, T_i, T_e, T_s) in the table. The plasma-ion and plasma-electron temperatures are not equal. For each day, the table shows:

(1) The relative strength of emission current to plasma current.

(2) The surface potential ϕ_o, negative or zero for all 4 days.

(3) Barrier potential (minimum) ϕ_{min}, according to measurement.

(4) Barrier potential if any $\phi_{min}(W)$, according to Whipple's method.

(5) Barrier potential if any $\phi_{min}(P)$, according to the exact theory of this report (computer program PARKSS).

(6) Barrier position if any $r_m(W)$, according to Whipple's method.

(7) Barrier position if any $r_m(P)$, according to PARKSS.

The results are as follows:

For Days 198, 199, and 204, the Whipple method predicts a barrier, while PARKSS predicts either no barrier (Day 198) or a smaller barrier (Days 199 and 204). For Day 273 both theories agree in predicting no barrier. In all cases, the measurements indicate the existence of a barrier and the depth of this barrier is greater than any of the predicted values. The discrepancy between theory and measurement is striking for Day 273, where the emission is cold and weak, and where the emitted electrons would be expected to roll downhill without building up a barrier. The potential distributions for the 4 problems are not shown here, but are typified by several of the profiles in Fig. 3, for zero and negative ϕ_o.

The numbers of iterations required for the 4 problems ranged from 40 to 60.

TABLE 2.

FLUXES: AMBIENT ONLY (MAXWELLIAN)

$$\lambda_D = .37$$

ϕ_0	j_i'	j_i	j_e
2	.135	.0032	2.77
1	.37	.0086	1.93
.8	.45	.011	1.76
.6	.55	.013	1.58
.4	.67	.016	1.39
.2	.82	.019	1.20
0.	1.00	.023	1.00
-.2	1.20	.028	.82
-.4	1.39	.032	.67
-.6	1.58	.037	.55
-.8	1.76	.041	.45
-1	1.93	.045	.37
-2[a]	2.77	.065	.135

[a] Equilibrium ϕ_0 below -2.

TABLE 3.

FLUXES: EMITTED ONLY (MAXWELLIAN)

$$\lambda_D = .37$$

φ_0	j_s	$\phi_{min}(r_m)$
2	.33	negligible
1	.63	-.013 (1.85)
.8	.70	-.041 (1.70)
.6	.76	-.082 (1.60)
.4	.82	-.14 (1.50)
.2	.88	-.20 (1.45)
0.	.92	-.28 (1.35)
-.2	.96	-.37 (1.25)
-.4	.99	-.49 (1.20)
-.6	1.00	-.62 (1.10)
-.8[a]	1.00	monotone
-.99	1.00	monotone

(a) Surface field nearly zero.

TABLE 4.

FLUXES: AMBIENT AND EMITTED (MAXWELLIAN)

$$\lambda_D = 0.37$$

ϕ_0	j_i'	j_i	j_e	j_s	$\phi_{min}(r_m)$
2	.135	.0032	2.61	.35	negligible
1	.37	.0086	1.80	.66	negligible
.8	.45	.011	1.64	.74	negligible
.6	.55	.013	1.47	.81	-.009 (1.95)
.4	.67	.016	1.31	.88	-.033 (1.75)
.2	.82	.019	1.15	.94	-.065 (1.55)
0. (a)	1.00	.023	.98	.98	-.12 (1.35)
-.2 (b)	1.20	.028	.82	1.00	-.22 (1.10)
-.4	1.40	.033	.67	1.00	monotone
-.6	1.60	.037	.55	1.00	monotone
-.8	1.79	.042	.45	1.00	monotone
-.99	1.97	.046	.37	1.00	monotone
-2.	2.86	.067	.135	1.00	monotone

(a) Equilibrium ϕ_0 slightly above 0.

(b) Surface field vanishes for ϕ_0 about -0.2.

-50-

TABLE 5.

FLUXES: MAXWELLIAN AMBIENT AND MONOENERGETIC EMITTED

$(T_i, T_e, T_s = 5, 5, 1 \text{ eV}; N_o, N_{so} = 1, 211/\text{cm}^3; r_o = 100 \text{ cm})$

ϕ_o	$j_i^{(a)}$	$j_e^{(a)}$	$j_s^{(a)}$	$\phi_{min}(r_m)$	$r(n_s=o)$
3	.000068	.0085	0.	monotone	1.28
2	.000083	.0074	0.	monotone	1.42
1.5	.000092	.0069	0.	monotone	1.55
1.075	.00010	.0064	0.	monotone	1.80
.99$^{(b)}$	.00010	.0063	.011	-.0072 (1.95)	-
.5	.00011	.0058	.58	-.27 (1.70)	-
0.	.00012	.0053	1.00	-.40 (1.55)	-
-.5	.00014	.0048	1.00	-.59 (1.28)	-
-1	.00015	.0043	1.00	monotone	-

(a) Ion mass = 1836 electron masses. All fluxes normalized by emission flux.

(b) Equilibrium ϕ_o slightly less than +1.0.

TABLE 6.

ATS 6 DATA AND THEORETICAL COMPARISONS

N_o = ambient density (cm^{-3})

N_{so} = photoelectron density (cm^{-3})

T_i = ambient-ion temperature (eV)

T_e = ambient-electron temperature (eV)

T_s = photoelectron temperature (eV)

ϕ_o = satellite potential (volts)

ϕ_{min} = barrier potential (volts)

r_m = barrier radius divided by $r_o = 5m$

$\phi_{min}(W)$ = barrier potential, Whipple approximation (1976)

$\phi_{min}(P)$ = barrier potential, Parker exact theory (PARKSS)

$r_m(W)$ = barrier radius, Whipple approximation (1976)

$r_m(P)$ = barrier radius, Parker exact theory (PARKSS)

Quantity	Day 198	Day 199	Day 204	Day 273
N_o	0.2	1.2	90	17
N_{so}	10.3	90	200	0.4
T_i	7	10	3.5	650
T_e	65	32	14.5	320
T_s	4.9	2	1.9	6
Relative strength of photoemission*	strong	strong	competitive	weak
ϕ_o	-20	0	-2	-2000
ϕ_{min}(measured)	-60	-10	-10	-2050
$\phi_{min}(W)$	-24.5	-6.2	-3.2	none
$\phi_{min}(P)$	none	-2.2	-2.5	none
$r_m(W)$	6	4	1.5	none
$r_m(P)$	none	1.5	1.2	none

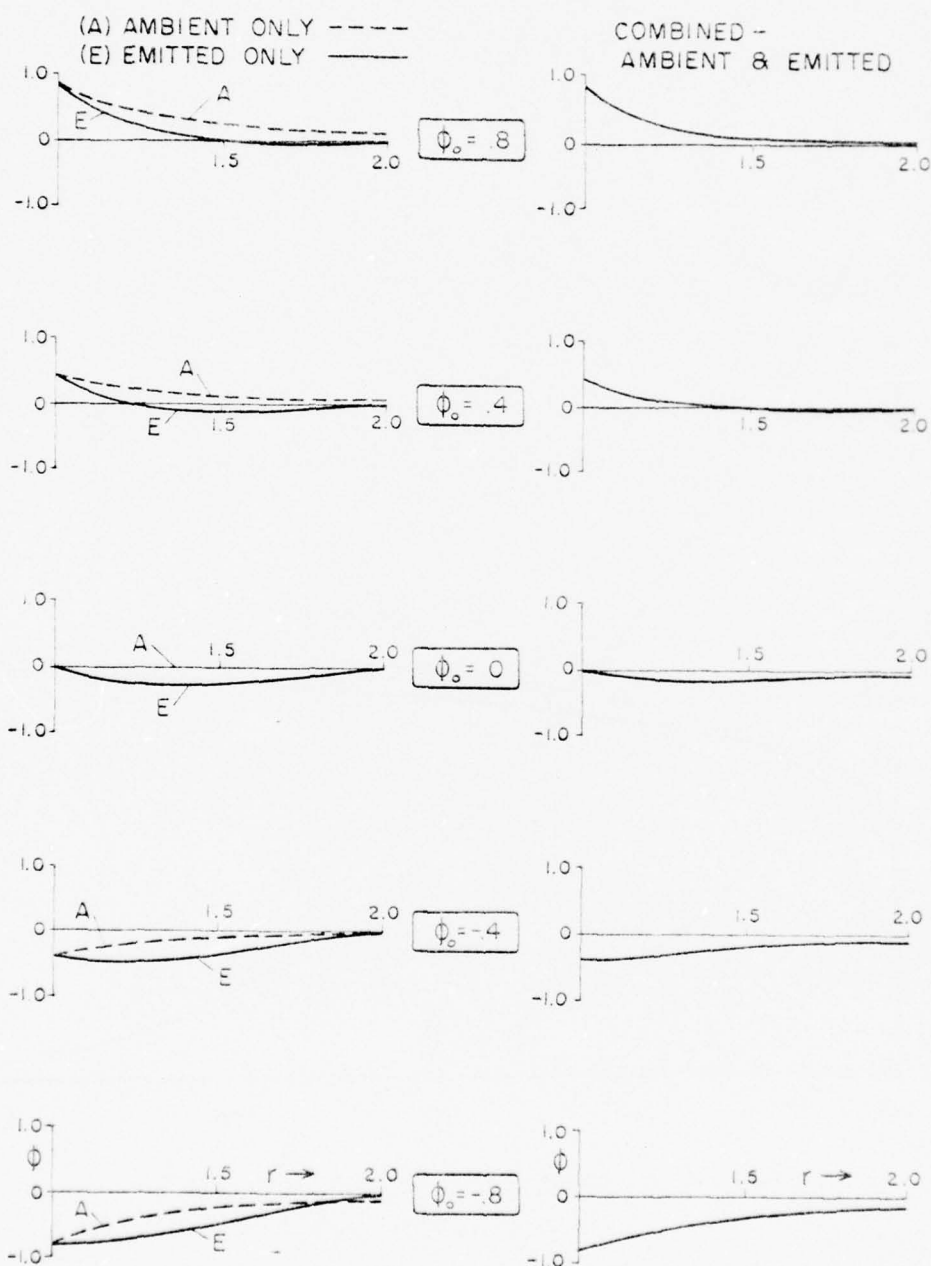* $N_{so}\sqrt{T_s}$ versus $N_o\sqrt{T_e}$

FIG. 3.   POTENTIAL PROFILES, MAXWELLIAN $\lambda_D = 0.37$
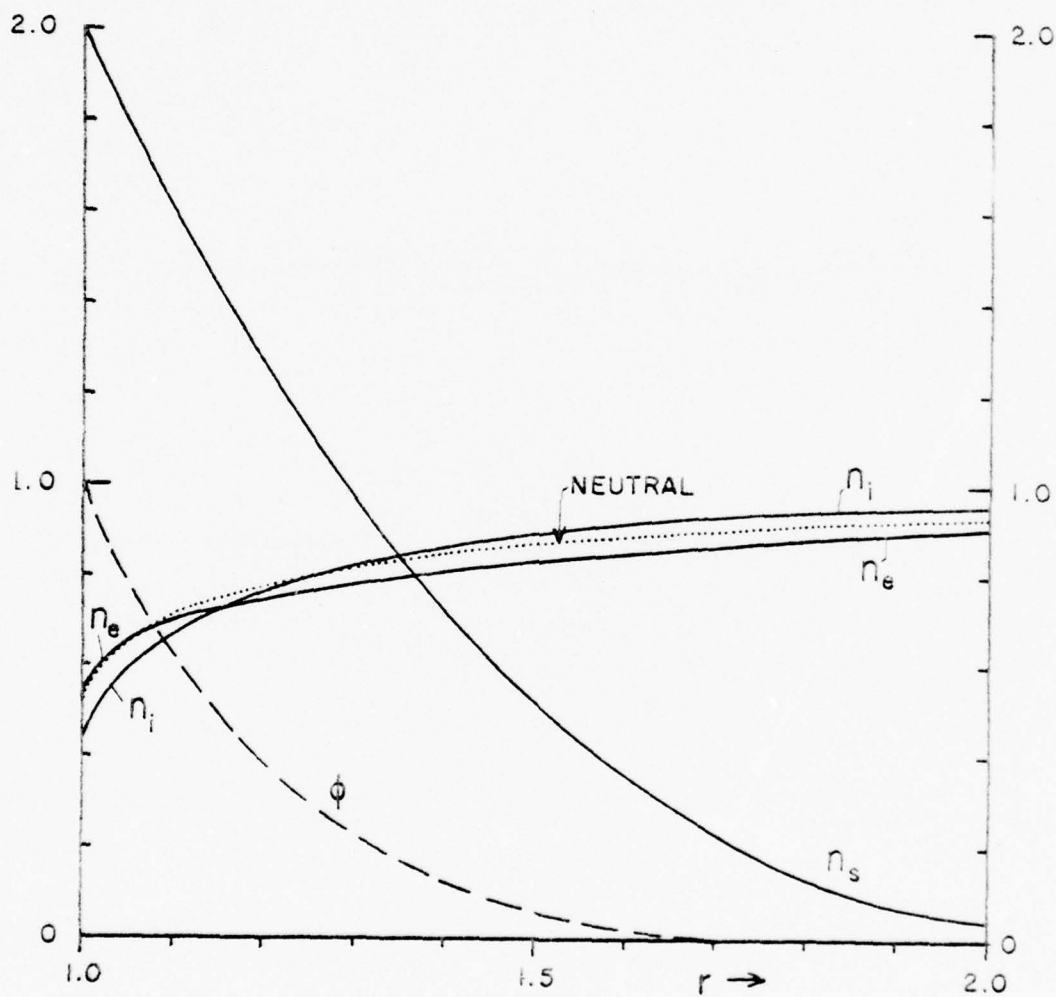
FIG. 4.   STRONG EMISSION, MONOENERGETIC
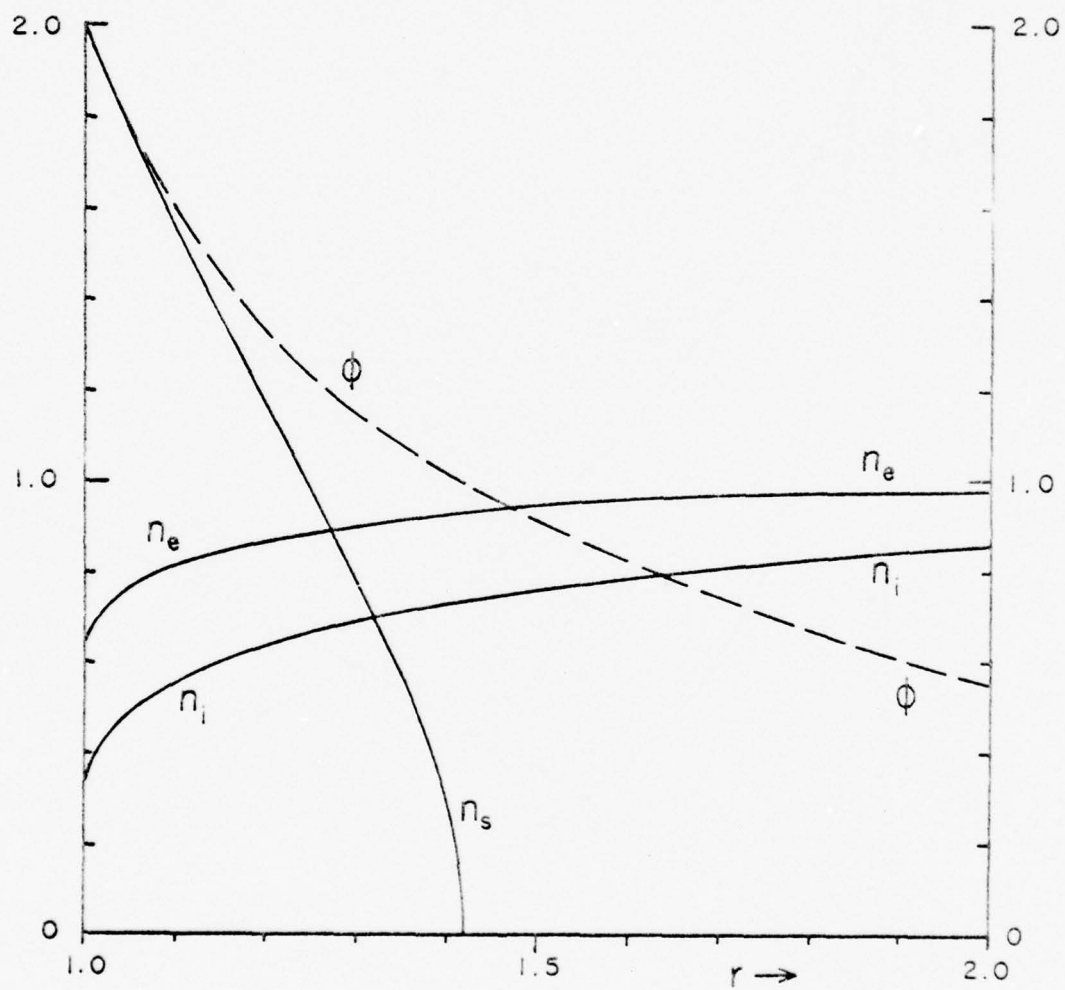Equilibrium Potential

FIG. 5.   STRONG EMISSION, MONOENERGETIC
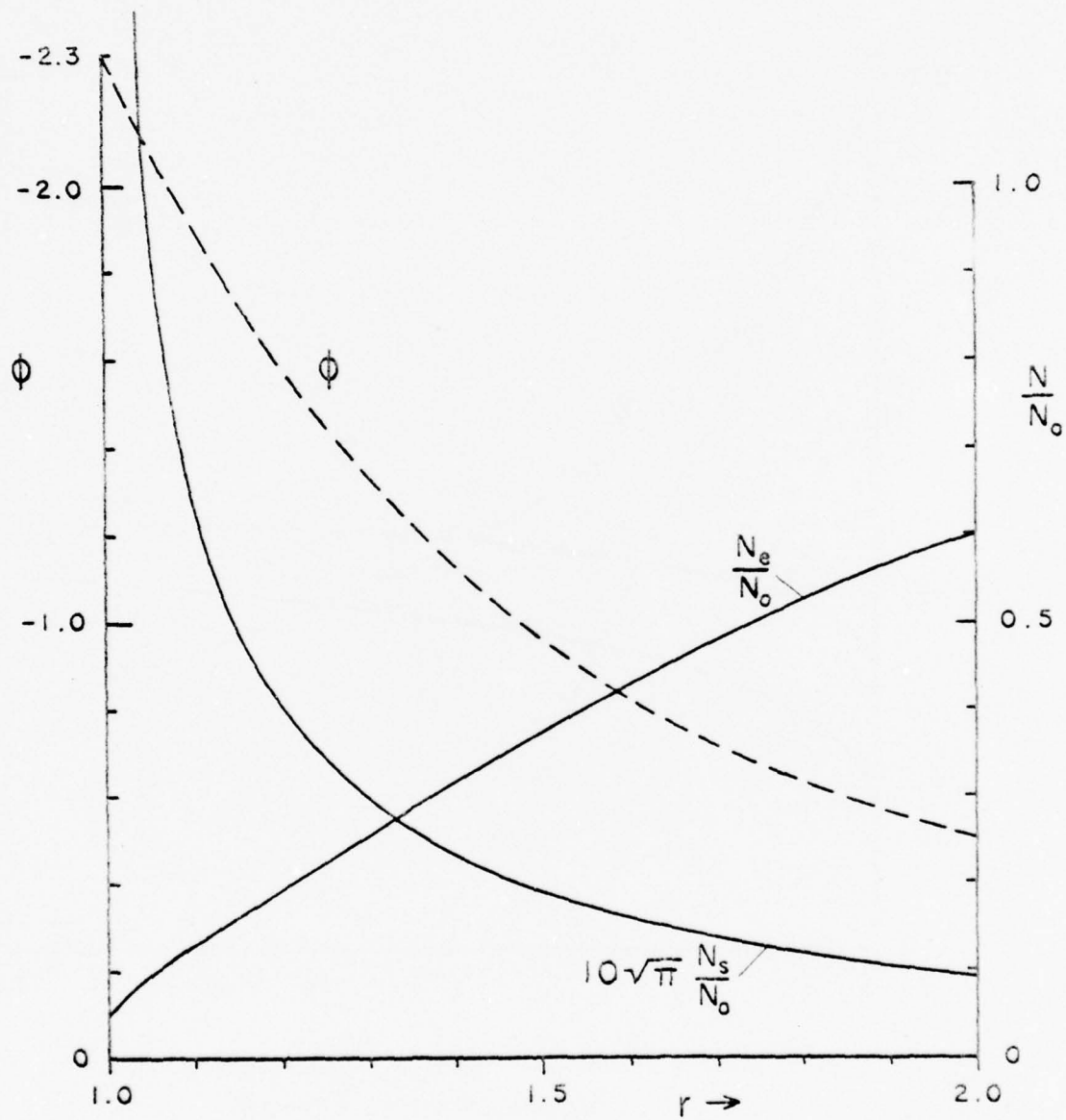Above-equilibrium Potential
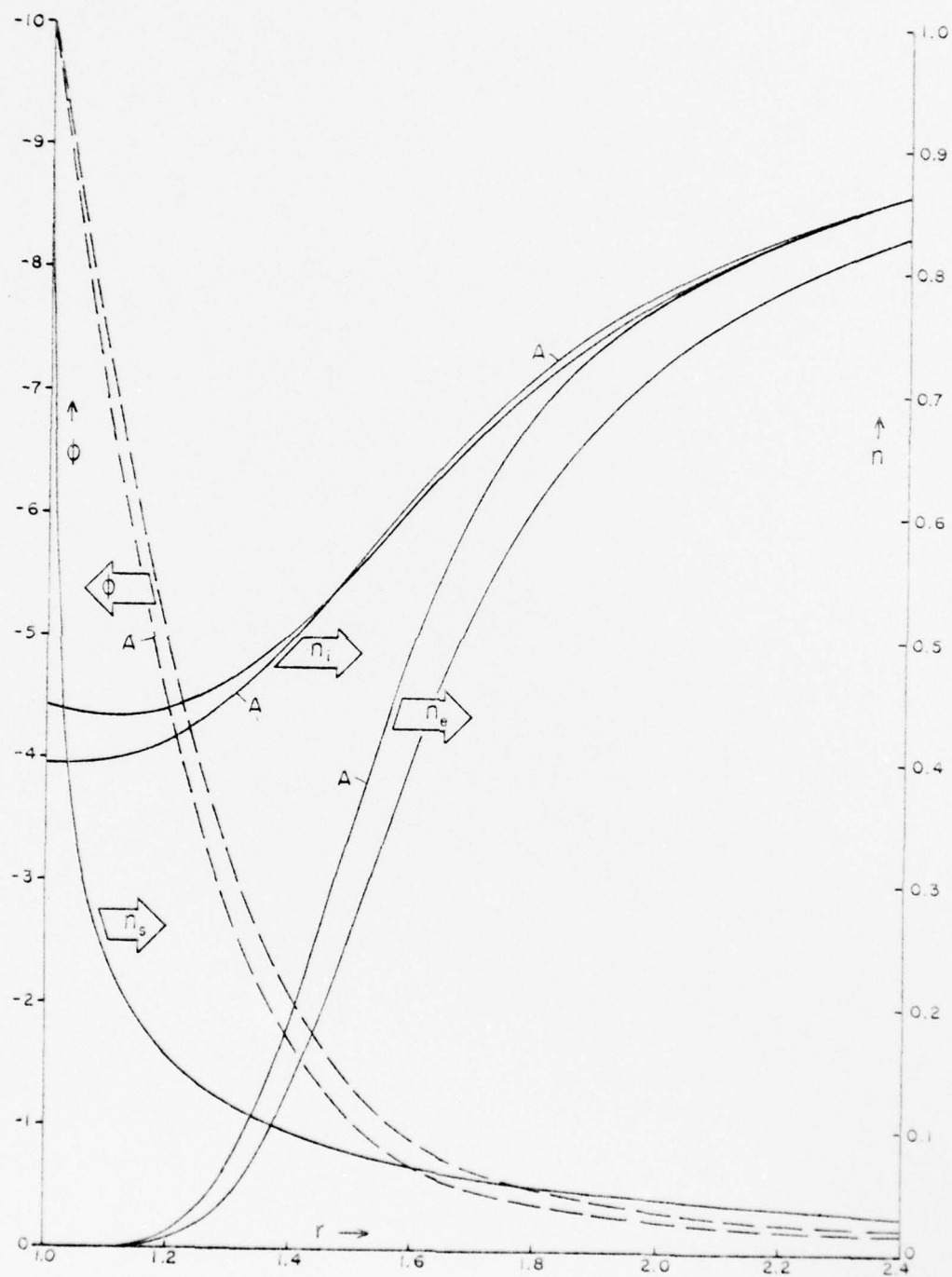
FIG. 6.   WEAK COLD EMISSION, MAXWELLIAN

FIG. 7.   SMALL DEBYE NUMBER λ_D=0.1, MAXWELLIAN
With and Without Emission (A=without)

-57-

APPENDIX A.

ENERGY QUADRATURE FORMULAS

The energy quadrature formulas used in this work have the form, appropriate to Maxwellian energy distributions:

$$(const) \int_{E_{min}}^{\infty} exp(-E)dE \cdot M(E) = \sum_{k=1}^{K} C_k \cdot M(E_k) \qquad (A-1)$$

where "const" denotes a constant multiplier, and where $M(E)$ is the monoenergetic factor depending on the energy E resulting from integration over J^2. C_k and E_k denote the coefficients and abscissas respectively of the K-th-order quadrature formula. The coefficients are evaluated by PARKSS as follows:

Given a potential distribution defined at a set of radial grid points r_i, there is an associated set of discrete potentials $\phi_i = \phi(r_i)$. Arrange the set of ϕ_i-values in order of increasing value. Then, if E_{min} of Eq. (A-1) is identified with the least value of the set of ϕ_i-values, and if E_{max} is identified with the greatest value of this set, we may split the integral and sum of Eq. (A-1) into two parts, one corresponding to the finite range (E_{min}, E_{max}), and the other to the semi-infinite range (E_{max}, ∞):

$$\int_{E_{min}}^{\infty} exp(-E)de \cdot M(E) = \int_{E_{min}}^{E_{max}} + \int_{E_{max}}^{\infty} exp(-E)dE \cdot M(E) \qquad (A-2)$$

where the const factor of Eq. (A-1) has been omitted.

First we consider the semi-finite range (second integral), and then the finite range (first integral).

A.1 Semi-Infinite Range

For the semi-infinite range we may employ quadrature formulas developed by Steen et al (1969), or by Laframboise and Stauffer (1969). These are

designed for the Maxwellian case where the integrand contains a Gaussian function as a weighting function. Let a_k, H_k denote an abscissa-coefficient pair from the data of Steen et al (1969). Then one transforms the semi-infinite range integral to

$$\int_{E_{max}}^{\infty} \exp(-E)dE \cdot M(E)$$

$$= \exp(-E_{max}) \int_{0}^{\infty} \exp(-U)dU \cdot M(U+E_{max})$$

$$= \sum_{k=1}^{N} 2H_k a_k \cdot M(a_k^2 + E_{max}) \qquad \text{(A-3)}$$

Here we have formed the k-th coefficient as $C_k = 2H_k a_k$, and the associated k-th energy abscissa as $E_k = a_k^2 + E_{max}$. The coefficients H_k and abscissas a_k may also be obtained from the "One-Dimensional" table of Laframboise and Stauffer if one multiplies their coefficients by $\sqrt{\pi}$ and their abscissas by unity. (There is also the option of using the Laframboise-Stauffer "Two-Dimensional" or "Three-Dimensional" abscissas and coefficients as they suggest for a cylindrical or spherical problem, respectively. However, it is the author's opinion based on experience with both methods that this yields no significant gain in practice.)

A.2 Finite Range

The finite range of energies (E_{min}, E_{max}) defined by the set of ordered values of ϕ_i consists of a number of unequal energy intervals. The number of such intervals is equal to the number of grid points minus one. Consider one of these intervals, and assume its energy range is (A,B). Then its contribution to the energy integral may be written

$$\int_A^B \exp(-E)dE \cdot M(E) = \int_0^{\sqrt{B-A}} \exp(-A-u^2) \cdot 2udu \cdot M(u^2+A)$$

$$= \sum_k C_k \cdot M(E_k = u_k^2 + A) \tag{A-4}$$

To obtain a given desired order of the quadrature formula, one may obtain from Eq. (A-4) a sequence of moment equations. For Order 2 as used in PARKSS, we have:

$$I_m = \int_0^{\sqrt{B-A}} \exp(-A-u^2) \cdot u^m \cdot 2udu = C_1 u_1^m + C_2 u_2^m \tag{A-5}$$

where $m = 0, 1, 2,$ and 3. Equations (A-5) constitute 4 equations for 4 unknowns: u_1, u_2, C_1, and C_2. The solution is as follows:

$$\begin{cases} u_1 = b - \sqrt{b^2 - a} \\ \\ u_2 = b + \sqrt{b^2 - a} \end{cases} \tag{A-6}$$

$$\begin{cases} b = 0.5(I_0 I_3 - I_1 I_2)/(I_0 I_2 - I_1^2) \\ \\ a = (I_2^2 - I_1 I_3)/(I_1^2 - I_0 I_2) \end{cases} \tag{A-7}$$

$$\begin{cases} C_1 = 2u_1 \exp(-A)(I_1 - I_0 u_2)/(u_1 - u_2) \\ \\ C_2 = 2u_2 \exp(-A)(I_1 - I_0 u_1)/(u_2 - u_1) \end{cases} \tag{A-8}$$

where

$$I_0 = \frac{\sqrt{\pi}}{2} \, erf(\sqrt{B-A})$$

$$I_1 = 0.5(1-exp(A-B))$$

$$I_2 = 0.5(I_0-\sqrt{B-A} \, exp(A-B))$$

(A-9)

$$I_3 = I_1 - 0.5(B-A) \, exp(A-B)$$

It may be noted that replacing B by infinity and A by zero in the above equations yields the abscissas and coefficients of Steen et al for Order 2.

For small (B-A), one may expand the foregoing equations to obtain the lowest order:

$$C_1 = C_2 = C \cong 0.5\sqrt{B-A}$$

$$u_1 \cong (1-1/\sqrt{3})C$$

(A-10)

$$u_2 \cong (1+1/\sqrt{3})C$$

After computing the u's and C's as above, one forms the coefficients and energies used in PARKSS by:

$$E_1 = u_1^2 + A$$

$$E_2 = u_2^2 + A$$

(A-11)

$$C_1 = (const)C_1$$

$$C_2 = (const)C_2$$

where the const factor is that on the left-hand side of Eq. (A-1).

One may choose an order M higher than 2 for any energy interval, in which case the 4 equations, Eq. (A-5), are replaced by 2M simultaneous equations. However, the additional computer time required may not be justified.

APPENDIX B.
LIMIT OF COLD EMISSION FROM NEGATIVE PROBE

We first derive the expression for the density of emitted particles when the potential is repulsive ($\phi > 0$) and monotonic. (Here, ϕ denotes the potential divided by $-|kT_s/e|$; thus, this applies to electrons emitted from a negative probe having dimensionless potential $+\phi_0$ with reference to electrons.) If the emission is weak the floating potential referred to ions will normally be negative (positive when referred to electrons) and the profile will be monotonic.

Consider the turning-point function $g \equiv r^2(E-\phi)$. In the above situation, ϕ is a positive and monotonically decreasing function of r, and $E > \phi$, so that g also rises monotonically. For $E < \phi_0$, we have $g < 0$ at $r = 1$; hence there can be no emitted contributions. For $E > \phi_0$ we have the least value of g, $g = E - \phi_0$, occurring at $r = 1$. Thus, there are only Type-1 orbits (Sec. 6) occupiable by emitted electrons, and so we may use Eq. (56) with $J_1^2 = E - \phi_0$. In view of Eqs. (26) and (33) for the spherical and cylindrical density, respectively, Eqs. (53)-(56) yield:

$$M_{ns}(E) = \sqrt{E-\phi} - \sqrt{E-\phi-(E-\phi_0)/r^2} \qquad (B-1)$$
(sphere)

$$M_{nc}(E) = \frac{2}{\pi}\sin^{-1}\sqrt{\frac{E-\phi_0}{r^2(E-\phi)}} \qquad (B-2)$$
(cylinder)

Substituting Eq. (B-1) into Eq. (25) (where ϕ_s is replaced by ϕ_0) and integrating from ϕ_0 to infinity yields for the spherical density due to a Maxwellian distribution of emitted particles:

$$\frac{N_s}{N_{so}} = ER(\phi_0-\phi) - \sqrt{1-1/r^2}\ ER\left\{\frac{r^2(\phi_0-\phi)}{r^2-1}\right\} \qquad (B-3)$$

where $ER(x) \equiv \exp(x) \cdot \text{erfc}\sqrt{x}$.

A similar substitution of Eq. (B-2) into Eq. (32) for the cylindrical problem results in:

$$\frac{N_s}{N_{so}} = \frac{2}{\pi} \int_0^{\infty} \exp(-u) du \cdot \sin^{-1} \sqrt{u/r^2(u+\phi_0-\phi)} \qquad (B-4)$$

which cannot be expressed in terms of elementary functions.

For monoenergetic emission, we substitute $1+\phi_0$ for E in Eqs. (B-1) and (B-2) so that

$$\frac{N_s}{N_{so}} = \sqrt{1+\phi_0-\phi} - \sqrt{1+\phi_0-\phi - 1/r^2} \qquad (B-5)$$
(monoenergetic, sphere)

and

$$\frac{N_s}{N_{so}} = \frac{2}{\pi} \sin^{-1} \sqrt{\frac{1}{r^2(1+\phi_0-\phi)}} \qquad (B-6)$$
(monoenergetic, cylinder)

Now proceeding to the limit of cold emission, we let $\phi_0-\phi$ become large compared with unity. Then Eq. (B-3) is replaced by

$$\frac{N_s}{N_{so}} \approx \frac{1}{\sqrt{\pi}r^2(\phi_0-\phi)} \qquad \text{(sphere, Maxwellian)} \qquad (B-7)$$

Equation (B-4) is replaced by

$$\frac{N_s}{N_{so}} \approx \frac{\sqrt{\pi}}{r\sqrt{\phi_0-\phi}} \qquad \text{(cylinder, Maxwellian)} \qquad (B-8)$$

-B2-

Equation (B-5) is replaced by

$$\frac{N_S}{N_{SO}} = \frac{1}{2r^2(\phi_0 - \phi)} \qquad \text{(sphere, monoenergetic)} \qquad \text{(B-9)}$$

And Eq. (B-6) is replaced by

$$\frac{N_S}{N_{SO}} = \frac{2}{\pi r \sqrt{\phi_0 - \phi}} \qquad \text{(cylinder, monoenergetic)} \qquad \text{(B-10)}$$

These limiting formulas are identical to those which would result from the assumption of purely radial motion, with no initial kinetic energy. That is, the electrons roll downhill after essentially starting from "rest".

APPENDIX C.

COMPUTER PROGRAM PARKSS

The following FORTRAN listing is for the PARKSS computer program.

```
      PROGRAM PARKSSG(INPUT,OUTPUT,TAPE60=INPUT,TAPE61=OUTPUT)
C
C     SPHERICAL SATELLITE - SHEATH DUE TO AMBIENT PLASMA
C                       AND SURFACE-EMITTED ELECTRONS
C     (PARKSSG) = PARKER METHOD FOR SPHERICAL SHEATH GENERALIZED.
C
C     L. W. PARKER, LEE W. PARKER, INC.
C            252 LEXINGTON ROAD, CONCORD, MASS.  JUNE 1974.
C
C     PHI(1)= SPHERE POTENTIAL (NEGATIVE FOR ION ATTRACTION).
C     BASED ON AMBIENT-ELECTRON TEMPERATURE IF KASE=0 .
C     BASED ON EMITTED-ELECTRON TEMPERATURE IF KASE=3 .
C     DEYE= DEBYE NUMBER (RATIO OF DEBYE LENGTH TO SPHERE RADIUS)
C     =AMBIENT-ELECTRON DEBYE NUMBER IF KASE=0.
C     =EMITTED-ELECTRON DEBYE NUMBER IF KASE=3.
C     TRATIO= RATIO OF
C     EMITTED-ELECTRON TEMPERATURE TO AMBIENT-ELECTRON TEMPERATURE IF KASE=0.
C     AMBIENT-ELECTRON TEMPERATURE TO EMITTED-ELECTRON TEMPERATURE IF KASE=3.
C     ORATIO= RATIO OF
C     EMISSION DENSITY TO AMBIENT DENSITY IF KASE=0.
C     AMBIENT DENSITY TO EMISSION DENSITY IF KASE=3.
C     TITE= RATIO OF AMBIENT-ION TEMPERATURE TO AMBIENT-ELECTRON TEMPERATURE
C     MIME= RATIO OF ION MASS TO ELECTRON MASS.
C     RB= OUTER RADIAL BOUNDARY IN UNITS OF SPHERE RADIUS.
C     ALPHA= ITERATION PARAMETER
C     NMP= NUMBER OF MESH POINTS = NUMBER OF RADIAL INTERVALS PLUS ONE
C     ME=0 FOR MONOENERGETIC PARTICLES
C     ME.GT.0 FOR MAXWELLIAN PARTICLES
C     KASE=1 FOR EMITTED ELECTRONS ONLY
C     KASE=2 FOR AMBIENT PLASMA ONLY
C     KASE= 0 OR 3 FOR BOTH AMBIENT PLASMA AND EMITTED ELECTRONS.
C     PRINT= NUMBER OR ITERATION STEPS BETWEEN ONE-LINE OUTPUTS.
C     MINP=0  FULL OUTPUT (NMP LINES) WHEN TIME TO PRINT.
C     MINP=1  MINIMUM OUTPUT (ONE LINE) WHEN TIME TO PRINT.
C     ABC=0.  ZERO-POTENTIAL BOUNDARY CONDITION
C     ABC=1.  ZERO-GRADIENT BOUNDARY CONDITION
C     ABC=-1. INVERSE-SQUARE-LAW BOUNDARY CONDITION
C     ABC=-2. COULOMB-LAW BOUNDARY CONDITION
1000  FORMAT(E15.5,I5,I4,I1)
1024  FORMAT(5H1PHI(1)=,F16.6,5X,27H1S SPHERE POTENTIAL BASED ON ,A9,
     1 20HELECTRON TEMPERATURE/
     2 1X,7HDEBYE =,F16.6,5X,3H1S ,A9,21HELECTRON DEBYE NUMBER/
     3 1X,7HRATIO =,F16.6,5X,10H1S RATIO OF ,A9,24HELECTRON TEMPERATURE
     4TO ,A9,23HELECTRON TEMPERATURE/
     5 1X,7HORATIO=,F16.6,5X,14H1S RATIO OF ,A9,11HDENSITY TO ,A9,
     6 7HDENSITY/
     7 1X,7HTITE  =,F16.6,5X,57H1S RATIO OF AMBIENT-ION TEMPERATURE TO A
     8MBIENT-ELECTRON TEMPERATURE)
1025  FORMAT(1X,3HME=,I3,3X,5H1MIME=,F5.1,5X,5HMME=,3HSE=,I2)
1026  FORMAT(1X,33HKASE=1 FOR EMITTED ELECTRONS ONLY )
1027  FORMAT(1X,30HKASE=2 FOR AMBIENT PLASMA ONLY )
1028  FORMAT(1X,43HBOTH AMBIENT PLASMA AND EMITTED ELECTRONS,5X,5HKASE=,
     1 I2)
1050  FORMAT(16H1ITERATION NUMBER ,I5,5X,21HCHANGE IN POTENTIAL =,
     1 1PE12,4X,21HCHANGE IN CURRENT =,E12,4X,7H1NO.=,7E12/
     2 1X,21HAMBIENT-ION CURRENT =,E16.8)
```

PARKSSG

```
     3 5X,27HAMBIENT-ELECTRON CURRENT =,E16.8,
     4 4X,25HEMITTED-ELECTRON CURRENT =,E16.8/
1051  FORMAT(1X,13HTIMES DSQRT TIMES SQRT(TITE/MIME),
     1 5X,5HGIVES,E11.4,21H AMBIENT-ION CURRENT=DSQRT/
     2 1X,5HGIVES,E11.4,24H AMBIENT-ELECTRON CURRENT/
     3 1X,5HGIVES,E11.4,26H EMITTED-ELECTRON CURRENT/
     4 1X,36HRELATIVE TO AMBIENT-ELECTRON CURRENT.
     5 5X,34HRELATIVE TO NORMAL AMBIENT-ELECTRON CURRENT)
1052  FORMAT(1X,13HTIMES DSQRT TIMES SQRT(TITE/MIME),
     1 4X,5HTIMES,1PE11.4,27H=ORATIO*SQRT*RATIO=DSQRT/
     2 1X,5HGIVES,E11.4,21H AMBIENT-ION CURRENT,
     3 1X,34HGIVES,E11.4,26H AMBIENT-ELECTRON CURRENT,
     4 1X,36HRELATIVE TO AMBIENT-ELECTRON CURRENT.
     5 5X,34HRELATIVE TO NORMAL AMBIENT-ELECTRON CURRENT)
1053  FORMAT(1X,1HI,5X,1HR,6X,3HPHI,3X,5H3TAB=I1,4X,5HOTAB=E1,7X,
     1 10H(EMITTED),2X,2HNET CH-DEN,1X,5HIONS=E1,4X,5H(ANB-E),3X,
     2 10H(EMITTED),3X,16HNET CH-DEN (OLD)//
     3 11X,I5,2X,0PF7.4,1PE12.4))
1054  FORMAT(1X,1PE11.4,21H AMBIENT-ION CURRENT/
     1 1X,5HGIVES,E11.4,21H AMBIENT-ION CURRENT,
     2 1X,7HRELATIVE TO ,A7,17H-ELECTRON CURRENT)
1075  FORMAT (1H0/3HSOLUTION DOES NOT SATISFY CONVERGENCE CRITERIA,
     1 5X,6HEPS=1PE8.1)
1100  FORMAT(3H0/30HSOLUTION SATISFIES CONVERGENCE,ACE CRITERIA,5X,
     1 6HEPS=1PE8.1,5X,7HCHANGE IN CURRENT LT EPS X 100 AT IT=I5)
1175  FORMAT(11X,3HCHANGE IN ,5X,13HMAX CHANGE,4X
     1 13HAMBIENT-ION,2X,16HAMBIENT-ELECTRON,1X,16HEMITTED-ELECTRON/
     2 4X,2HIT,4X,9HPOTENTIAL,5X,3H=NM=IN CURRENT,5X,3HA,
     3 5X,7HCURRENT,5X,7HCURRENT,1G4,7HC-AREA//)
1150  FORMAT (1H4,I4,1PE16.4,3E16.4)
C
C
      COMMON PHI(201),X(201,3),Y(201,3),R(201),PSI(201),ROUT(201),
     1 CUR(1),COEFD(500),COEFC(500),EE(500),
      COMMON/E1/ IPRINT,IPRENT,PR,ME,XRAY,KASE,TRATIO,PHIMAX,TITE
      INTEGER CC,PRINT,PRPR
      REAL MIME
      DIMENSION F(201),W0(201),AI(201,3),R1(201),PSI1(201),ZETA(201),
     1 F1(201),FP1(201),GMINPK(3),GMINPK(3)
      EQUIVALENCE (PSI,ZETA)
C
      DATA ITMAX,EPS/ 1000,1.3E-5/
C
      I=63
      PR=61
      IPRINT=1
      IPRENT=0
      PRINT=1
      PRINT=0
      MINP=1
      MINP=0
      ABC=0.
      ABC=1.
      TITE=1.
      MIME=1836.
      TRATIO=ORATIO=1.
200   READ(I,1000) PHI(1),DEBYE,TRATIO,ORATIO,TITE,RB,ALPHA,NMP,ME,KASE
```

3

PARKSSG

```
      IF(EOF(I)) 1,2
1     CALL EXIT
2     CONTINUE
      PART1=7HAMBIENT
      IF(KASE.EQ.3) PART1=7HEMITTED
      AMHI0=EMDINI
      EMI(1)=ME*ISSE10+
      IF(KASE.EQ.0) PART1=ANBT
      IF(KASE.EQ.0) PART2=EMIS
      IF(KASE.EQ.1) PART1=PART2=EMIS
      IF(KASE.EQ.2) PART1=PART2=ANBT
      IF(KASE.EQ.3) PART1=EMIS
      IF(KASE.EQ.3) PART2=ANBT
      WRITE(NM,1024)PHI(1),PART1,DEBYE,RB,PART1,
     1 TRATIO,PART2,PART1,ORATIO,PART2,PART1,TITE
      WRITE(NM,1025) RB,ALPHA,NMP,ME
      IF(KASE.EQ.1) ABC=0.
      IF(KASE.EQ.1) WRITE(NM,1026)
      IF(KASE.EQ.2) WRITE(NM,1027)
      IF(KASE.NE.1.AND.KASE.NE.2) WRITE(NM,1028) KASE
      CUR(1)=GMINPK=0.
      DSQRT=1.
      IF(KASE.EQ.0) DSQRT=2.*ORATIO*SQRT(TRATIO)
      IF(KASE.EQ.3) DSQRT=1.5*ORATIO*SQRT(TRATIO)
      WRITE(NM,1050)
      NM1=NMP-1
      NM2=NMP-2
      SABC=0.0
      IF (ABC.NE.0.0) GO TO 235
230   NF1=NM1
      NB1=NM2
      GO TO 240
235   SABC=ABC
      ABC=0.1
      P(1)=NMP=0.0
      GO TO 230
240   I=X
      RB(RX=1.)/FLOAT(NM1)
      R(1)=Y
250   DO 325 N=1,NMP
      F(N)=P(1)=NP=9.
      F1(N)=F(N)
      PHI(N)=FLOAT(N-1)*H
      ROOT(N)=R0.
      IF(N.GT.1) ROOT(N)=SQRT(1.-TR(1)/R(N))**2)
      R0(N)=PHI(N)**2
      NP(N)=NS*PHI(N)
      IF(DEBYE.GT.0.) NS(NS)=NS*R(N)/DEBYE**2
      DO 320 M=1,3
      ZE(M,N)=1.
      GEN(M)=0.0
      GMINPK(M)=0.
320   CONTINUE
325   CONTINUE
      PK(1)=PHI(N)*R(1)
C
C     RETURN FROM 685=1 OR 685=9 IF ABC.NE.0.AND.    IT=1
```

4

PARKSSG

```
C
C     A MATRIX DEFINED AND FACTORED
C
350   R(2,1)=X=2.
375   DO 400 I=3,NFS
      IN(1)=I-1
      A(IN(1,3)=1.0/X(IN1,1)
      A(1,1)=A(2,1)+A(IN1,2)
      IF (I.EQ.NMP)
      XA(NMP,2)=A-2.0*(1.0        -ABC*H/R(NMP)=2.0*X(IN1,2))
400   CONTINUE
C     ITERATION TO FIND PHI
      GMINPK=0.0
      ITRA=
      PRPA=0
      ICDS=3
430   DO 690 IT=1,ITMAX
433   DO 435 I=1,NMP
      FP(I)=F(I)
435   CONTINUE
      CC=0
      IF (IT.EQ.1) CC=1
C     SOLUTION OF THE LINEAR SYSTEM A*(PSI)=X
450   DO 500 I=2,NM1
      ZETA(I)=(A*PSI(I)*F(I)-ZETA(I-1))/A(I,1)
500   CONTINUE
      IF (ABC.NE.0.0) ZETA(NMP)=(A(NMP)*F(NMP)-2.0*ZETA(NMP-1))/A(NMP,
     1 1)
      I=NB5+1
525   DO 550 INDEX=2,NB5
      I=I-1
      PSI(I)=ZETA(I)=A(I,2)*PSI(I+1)
550   CONTINUE
C
560   ROMA=0.0
565   DO 570 I=2,NFS
      IF (PSI(I).NE.0.0)
      ROMA=AMAX1(ROMA,ABS(ABS(PSI(I))/PSI(I))=1.)))
570   CONTINUE
      IF (PRPA.EQ.1.AND.ICDS.EQ.1) GO TO 625
575   DO 625 I=1,NMP
      IF(CC.EQ.1 .OR. PSI(I).EQ.0.) GO TO 625
      IF(ABS(ABS(PSI(I))/PSI(I)))=1.0).LE.EPS) CC=1
620   PSI(I)=PSI(I)
610   PHI(I)=PSI(I)/R(I)
625   CONTINUE
      IF (CC.EQ.0) ICDS=1
626   CONTINUE
      IF(CC.EQ.0) WRITE(NM,1175) IP,ROMA,GROMA,CUR,I5,I5,CUR,I15
      CALL TIME(
650   DO 675 I=1,NMP
      IF(KASE.EQ.0) F(I)=ORATIO*DE(1,I) + DE(1,2)=DE(1,I)
      IF(KASE.EQ.2) F(I)=DE(1,3)
      IF(KASE.EQ.3) F(I)=DE(1,3)*5. + D(1,1)*DE(1,2)=DE(1,1)
      F(I)=ALPHA*F(I)+(1.-ALPHA)*F(I)
      F1(I)=F(I)
```

```
675 CONTINUE
    CUR1=SQRT(EEITG/MI*EAR      CUR(I))
    IF(KASE.EQ.2) CUR2=DSQRT*CUR(3)
    IF(KASE.EQ.3) CUR2=DSQRT*CUR(2)
    IF(KASE.EQ.3) CUR1=DSQRT*CUR1
    A=X*G
    JP=MYAR,
    DO 680 M=1,3
    X=CUR(M)
    Y=GMIN*PA(M)
    IF(X.NE.0..OR.Y.NE.0.) GO TO 678
    GRDMAX(M)=0.
    GO TO 680
678 GRDMAX(M)=X*2.*ABS(I)*Y/(X+Y))
    IF(GRDMX.LT.GRDMAX(M)) MSV=M
    IF(GRDMX.LT.GRDMAX(M)) GRDMX=GRDMAX(M)
680 CONTINUE
    IF(IT.LE.10) WRITE(MM,1150) IT,RDMX,GRDMX,MSV,(CUR(M),M=1,3)
    IF (GRDMX.LT.EPS*100.0.AND.ITG.EQ.0) ITG=IT
    IF(IT.GT.210.AND.GRDMX.GT.0.04) GO TO 780
    DO 682 M=1,3
682 GMIN=PA(M)=CUR(M)
    IF(ISAPC.EQ.0.0) GO TO 685
    ABC=CABC
    SABC=0.0
    SF=GMMP
    N=T*ARM)
    WRITE(MM,1150) IP,RDMX,GRDMX,MSV,(CUR(M),M=1,3)
    IF(KASE.EQ.0) WRITE(MM,1151) DSORT,CUR1,CUR3
    IF(KASE.EQ.3) WRITE(MM,1152) DSORT,CUR1,CUR2
    IF(KASE.EQ.2) WRITE(MM,1154) CUR1,PART
    WRITE(MM,1151)
    1 (I,R2(I),PHI(I),(DE(I,J),J=1,3),F(I),(G(I,J),J=1,3),FP(I),I=1,NMP)
C
C CONTINUE WITH ITERATION, RE-STARTING WITH ZERO-POTENTIAL-B.C. SOLUTION.
    GO TO 350
C
685 IF(MOD(IP,PRINT).NE.0.AND.CC.NE.0.AND.PPA.EQ.0.AND.IP.GT.1)
    1 GO TO 640
    WRITE(MM,1150) IP,RDMX,GRDMX,MSV,(CUR(M),M=1,3)
    IF(CC.EQ.0) GO TO 686
    IF(ARC.EQ.0.AND.IP.EQ.1) GO TO 686
    IF(ARC.NE.0.AND.IP.LE.2) GO TO 686
    IF(IP.NP.1) GO TO 687
686 WRITE(MM,1050) IP,RDMX,GRDMX,MSV,(CUR(M),M=1,3)
    IF(KASE.EQ.3) WRITE(MM,1051) DSORT,CUR1,CUR3
    IF(KASE.EQ.3) WRITE(MM,1052) DSORT,CUR1,CUR2
    IF(KASE.EQ.2) WRITE(MM,1054) CUR1,PART
    WRITE(MM,1053)
    1 (I,R(I),PHI(I),(DE(I,J),J=1,3),F(I),(G(I,J),J=1,3),FP(I),I=1,NMP)
    IF (CC.EQ.0) GO TO 725
C
C EXIT FROM IT-LOOP IF CONVERGED
C
687 PPPA=PPA+1
    GO TO 1X11,6881,PPPA
688 PPPA=0
```

```
689 CONTINUE
720 WRITE(MM,1075) EPS
    WRITE(MM,1050) IP,RDMX,GRDMX,MSV,(CUR(M),M=1,3)
    IF(KASE.EQ.0) WRITE(MM,1051) DSORT,CUR1,CUR3
    IF(KASE.EQ.3) WRITE(MM,1052) DSORT,CUR1,CUR2
    IF(KASE.EQ.2) WRITE(MM,1054) CUR1,PART
    WRITE(MM,1053)
    1 (I,R(I),PHI(I),(DE(I,J),J=1,3),F(I),(G(I,J),J=1,3),FP(I),I=1,NMP)
    GO TO 740
725 WRITE(MM,1100) EPS,ITG
740 CONTINUE
    GO TO 200
    END
```

```
                SUBROUTINE DENSE
C
C DENSITY PROGRAM
C PHI-DISTRIBUTION IS ARBITRARY
C
    COMMON P4I(201),G4201,3),DE(201,3),R(201),RSQ(201),R00YR(201),
    1 CUR(3),COEFD(500),COEFC(500),EE(500),
    COMMON/C1/ SPRINT,IT,NMP,MM,AE,PHAX,KASE,IFATIO,PHIMAX,IEFE
    DIMENSION PHISAVE(201),GMINSV(500),IRIGHT(500),ILEFT(500),DMPRI(500)
C
C SAVE POTENTIALS FOR SCALING
C
    DO 100 I=1,NMP
100 PHISAVE(I)=PHI(I)
C
C PARTICLE-TYPE LOOP
C (IP=1,2 FOR AMBIENT IONS, ELECTRONS, IP=3 FOR SURFACE ELECTRONS.)
C
    IPMIN=1
    IPMAX=1
    IF(KASE.EQ.1) IPMIN=3
    IF(KASE.EQ.2) IPMAX=2
C
    DO 600 IP=IPMIN,IPMAX
C
C SCALE POTENTIALS ACCORDING TO TYPE OF PARTICLE, AND FIND PHIMAX
C
    PHIMAX=-1.E77
    DO 200 I=1,NMP
    IF(I.EQ.1) CUR(IP)=0.
    DF(I,IP)=0.
    IF(KASE.EQ.1)              PHI(I)=PHISAVE(I)
    IF(KASE.EQ.2.AND.IP.EQ.2) PHI(I)=-PHI(I)
    IF(KASE.EQ.0.AND.IP.EQ.1) PHI(I)=-PHI(I)
    IF(KASE.EQ.0.AND.IP.EQ.3) PHI(I)=PHISAVE(I)/TRATIO
    IF(KASE.EQ.3.AND.IP.EQ.1) PHI(I)=PHISAVE(I)/TRATIO
    IF(KASE.EQ.3.AND.IP.EQ.2) PHI(I)=PHISAVE(I)/TRATIO
    IF(KASE.EQ.3.AND.IP.EQ.3) PHI(I)=PHISAVE(I)
    IF(IP.EQ.3) PHI(I)=PHI(I)/TI(I)
    IF(PHI(I).LE.PHIMAX) GO TO 200
    PHIMAX=PHI(I)
200 CONTINUE
    IF(PHIMAX.LT.0.) PHIMAX=0.
C
C COMPUTE COEFFICIENTS AND ENERGIES FOR ENERGY QUADRATURE
C
    CALL ENERGY(IP)
C
    DO 400 K=1,KMAX
C
    IF(IPRINT.EQ.0) GO TO 230
    DO 220 I=1,NMP
229 DI(I,IP)=RSQ(I)*(EE(K)-PHI(I))
    WRITE(MM,6000) K,II,GI(I,IP),I=1,NMP)
6000 FORMAT(I5,2H K,I2,2X,4H1,G+, 8(I3,1PE12.4)/(11X, 8(I3,E12.4)))
230 CONTINUE
```

```
C FOR EACH ENERGY, FIND MINIMUM (GMIN) OF G-FUNCTION
C STORE GMIN AND IRIGHT, ILEFT
C
    GMINSV(K)=-7.7777E+77
    GMIN=1.E+77
    ILEFT(K)=0
    IRIGHT(K)=NMP+1
    DO 100 I=1,NMP
    IF(IP.LE.2) I=NMP+1-J
    IF(IP.EQ.3) I=J
    GG=RSQ(I)*(EE(K)-PHI(I))
    IF(GG.GT.0.) GO TO 250
    IF(IP.LE.2) ILEFT(K)=I
    IF(IP.EQ.3) IRIGHT(K)=I
    GMIN=0.
    GO TO 100
250 IF(GG.GE.GMIN) GO TO 300
    GMIN=GG
300 CONTINUE
150 GMINSV(K)=GMIN
400 CONTINUE
    IF(IPRINT.GT.0)
    1 WRITE(MM,4000) (K,ILEFT(K),IRIGHT(K),GMINSV(K),K=1,KMAX)
4000 FORMAT(10X,1H,K,5X,5HILEFT,5X,6HIRIGHT,4X,4HGMIN/(1X,I10,2X,I10,
    1 1PE15.4))
C
    DO 700 I=1,NMP
C
C FOR EACH GRID POINT, SUM OVER ENERGIES AND ANGULAR MOMENTA
C
    DO 600 K=1,KMAX
    DMOND=0.
    DMPRI(K)=DMOND
    GMIN=GMINSV(K)
    IF(GMIN.LT.0.) GO TO 600
    IF(GMIN.GT.0.) GO TO 500
C
C FOR EACH ENERGY, IF GMIN=0, DETERMINE WHETHER THE ZERO IS ON THE
C WRONG SIDE OR RIGHT SIDE OF THE I-TH POINT
C
    IF(IP.LE.2.AND.I.LE.ILEFT(K)) GO TO 600
    IF(IP.EQ.3.AND.I.GE.IRIGHT(K)) GO TO 600
500 CONTINUE
C
C FIND LEAST VALUES (GN) OF G-FUNCTION, AHEAD OF AND BEHIND POINT I
C
    CALL MINIMA(IP,I,K,GN)
C
C INTEGRALS OVER ANGULAR MOMENTA TO YIELD MONOENERGETIC FACTORS
C (MONO FACTOR(I) OR XMIN (CURRENT))
C
    SMXID=ROOT1*ROOT1*0.
    IF(EE(K).LT.PHI(I)) GO TO 600
    SPFED=SQRT(EE(K)-PHI(I))
    GG=RSQ(I)*SMF**2
    IF(GG.LT.0.AND.GN.LT.0.) ROOT1=DSQRT(-GN/GG)
    IF(GG.GT.0.AND.GMIN.LT.GG) ROOT1=DSQRT(1.-GMIN/GG)
```

SUBROUTINE DENSE

SUBROUTINE ENERGY

SUBROUTINE ENERGY

SUBROUTINE ENERGY

```
      SUBROUTINE MINIMA(IP,IT,KK,GM)
C
C     FIND MINIMUM VALUES OF RSQ*(E-PHI), TO LEFT AND RIGHT OF II-TH PT.
C
      COMMON PHI(201),G(201,3),CF(201,3),R(201),RSQ(201),ROOTR(201),
     1 GIM(3),COEFD(500),COEFC(500),CE(500)
      COMMON/C1/ IPRINT,IT,NMP,MM,ME,XMAX,AASE,IRATIO,PHIMAX,TITE
C
      IF((IP.LE.2) GO TO 200
C
C     MINIMUM FOR I.LE.II (INNER REGION)
C
      GM=RSQ(1)*(EE(KK)-PHI(1))
      DO 100 I=1,IT
      GG=RSQ(I)*(EE(KK)-PHI(I))
      IF(GG.GT.2.) GO TO 50
      GM=0.
      RETURN
C
  50  IF(GG.GE.GM) GO TO 100
C
      GM=GG
 100  CONTINUE
      RETURN
C
C     MINIMUM FOR I.GE.II (OUTER REGION)
 200  GM=RSQ(NMP)*(EE(KK)-PHI(NMP))
      DO 300 I=II,NMP
      IREV=NMP+II-I
      GG=RSQ(IREV)*(EE(KK)-PHI(IREV))
      IF(GG.GT.0.) GO TO 250
      GM=2.
      RETURN
C
 250  IF(GG.GE.GM) GO TO 300
C
      GM=GG
 300  CONTINUE
      RETURN
      END
```

```
      SUBROUTINE SORT(STACK)
      COMMON/C1/ IPRINT,IT,NMP,MM,ME,XMAX,AATE,IRATIO,PHIMAX,TITE
      DIMENSION STACK(201)
C
C     ROUTINE TO ORDER ELEMENTS OF A VECTOR IN ORDER OF INCREASING VALUE
C
      KOUNT=1
  25  LOOPS=0
      DO 4 LOOP=1,2
      DO 1 I=LOOP,NMP,2
      IF(I.EQ.NMP) GO TO 1
      IF(STACK(I).LE.STACK(I+1)) GO TO 1
C
C     EXCHANGE IN PAIRS TO PUT IN ORDER OF INCREASING VALUE
C
      J=STACK(I)
      STACK(I)=STACK(I+1)
      STACK(I+1)=J
      LOOPS=1
   1  CONTINUE
   4  CONTINUE
      KOUNT=KOUNT+1
      IF(KOUNT.GT.10000) WRITE(MM,42) KOUNT
      IF(KOUNT.GT.10000) RETURN
  42  FORMAT( 26HWENT THROUGH LOOP MORE THAN ,I6,4H TIMES)
      IF(LOOPS.EQ.1) GO TO 25
      RETURN
      END
```

```
      REAL FUNCTION ERF(X)
C
C     ERROR FUNCTION
C
      DIMENSION A(7)
      DATA A,RPI /1.0,0.7052307AL,-1.0,42282012L,-1.0,9270622E-2,
     1 0.15201430E-3,0.27656720E-3,0.43063SC-4,1.772453B7/
 200  S=X**2
      R5=SORT(S)
      IF(X5.LT.4.) GO TO 240
 220  ERROR= 1.0/(R5*RPI)*(1.0+0.5/S*(-1.0+0.5/S*(1.0-7./S)))
      ERF=1.-ERROR*EXP(-S)
      RETURN
C
C     HASTINGS APPROXIMATION P.187
C
 240  SP=1.0
      SM=1.0
 250  DO 300 I=2,7
      SP=SP*RS
      SM=SM+A(I)*SP
      IF(ABS(SP).LT.1.0E-9) GO TO 350
 300  CONTINUE
 350  ERFC=1.0/SM**16
      ERF=1.-ERFC
      RETURN
      END
```

REFERENCES

1. Allen, J. E., R. L. F. Boyd, and P. Reynolds, The collection of positive ions by a probe immersed in a plasma, Proc. Phys. Soc. (London) B70, 297-304 (1957).

2. Bernstein, I. B., and I. N. Rabinowitz, Theory of electrostatic probes in a low-density plasma, Phys. Fluids 2, 112-121 (1959).

3. Bohm, D., E. H. S. Burhop, and H. S. W. Massey, The use of probes for plasma exploration in strong magnetic fields, in Characteristics of Electrical Discharges in Magnetic Fields, edited by A. Guthrie and R. K. Wakerling, Chap. 2, McGraw-Hill, New York (1949).

4. Chang, K. W., and G. K. Bienkowski, Effects of electron emission on electrostatic probes at arbitrary pressures, Phys. Fluids 13, 902-920 (1970).

5. Grard, R. J. L., K. Knott, and A. Pederson, The influence of photoelectron and secondary electron emission on electric field measurements in the magnetosphere and solar wind, in Photon and Particle Interactions With Surfaces in Space, edited by R. J. L. Grard, pp. 163-189, D. Reidel, Dordrecht, Netherlands (1973).

6. Laframboise, J. G., Theory of spherical and cylindrical Langmuir probes in a collisionless Maxwellian plasma at rest, UTIAS Rep. 100, Univ. of Toronto, Toronto, Ontario (June 1966).

7. Laframboise, J. G., and A. D. Stauffer, Optimum discrete approximation of the Maxwell distribution, AIAA J. 7, 520-523 (1969).

8. Medicus, G., Theory of electron collection of spherical probles, J. Appl. Phys. 32, 2512-2520 (1961).

9. Parker, L. W., Computer solutions in electrostatic probe theory, 1, spherical symmetry with collisions, Tech. Rep. AFAL-TR-72-222, Part 1, Air Force Avionics Lab, Wright-Patterson Air Force Base, Ohio (April 1973).

10. Parker, L. W., Computer method for satellite plasma sheath in steady-state spherical symmetry, Tech. Rep. AFCRL-TR-75-0410, Air Force Cambridge Research Labs, Hanscom Air Force Base, Massachusetts (July 1975).

11. Parker, L. W., and E. C. Sullivan, Iterative methods for plasma-sheath calculations - application to spherical probe, Tech. Rep. NASA Tech. Note D-7409, (March 1974).

12. Schröder, H., Spherically symmetric model of the photoelectron sheath for moderately large plasma Debye lengths, in Photon and Particle Interactions With Surfaces in Space, edited by R. J. L. Grard, pp. 51-58, D. Reidel, Dordrecht, Netherlands (1973).

13. Soop, M., Report on photo-sheath calculations for the satellite GEOS, Planet. Space Sci. 20, 859-870 (1972).

14. Steen, N. M., G. D. Byrne, and E. M. Gelbard, Gaussian quadratures for the integrals $\int_0^\infty \exp(-x^2)f(x)dx$ and $\int_0^b \exp(-x^2)f(x)dx$, Math. Comp. 23, 661-671 (1969).

15. Varga, R. S., Matrix Iterative Analysis, Prentice-Hall, Englewood Cliffs, New Jersey (1962).

16. Whipple, E. C., Jr., Theory of spherically symmetric photoelectron sheath: A thick sheath approximation and comparison with the ATS-6 observation of a potential barrier, J. Geophys. Res. 81, 601-607 (1976).

17. Whipple, E. C., Jr., and L. W. Parker, Effects of secondary electron emission on electron trap measurements in the magnetosphere and solar wind, J. Geophys. Res. 74, 5763-5774 (1969).